

# UC Irvine

## UC Irvine Electronic Theses and Dissertations

**Title**

Analysis and design of a stationary ring road with two signals

**Permalink**

<https://escholarship.org/uc/item/63z3m6kg>

**Author**

Shen, Shizhe

**Publication Date**

2016

Peer reviewed|Thesis/dissertation

UNIVERSITY OF CALIFORNIA,  
IRVINE

Analysis and design of a stationary ring road with two signals

THESIS

submitted in partial satisfaction of the requirements  
for the degree of

MASTER OF SCIENCE

in Civil Engineering

by

Shizhe Shen

Thesis Committee:  
Professor Wenlong Jin, Chair  
Professor Will Recker  
Professor R. Jayakrishnan

2016



# TABLE OF CONTENTS

	Page
<b>LIST OF FIGURES</b>	<b>iv</b>
<b>ACKNOWLEDGMENTS</b>	<b>v</b>
<b>ABSTRACT OF THE THESIS</b>	<b>vi</b>
<b>1 Introduction</b>	<b>1</b>
1.1 Background . . . . .	1
1.2 Traditional methods for signal design . . . . .	2
1.2.1 Cycle length . . . . .	2
1.2.2 Delay . . . . .	4
1.2.3 Signal coordination . . . . .	6
1.3 New methods for signal design . . . . .	8
<b>2 Problem statement</b>	<b>10</b>
2.1 The LWR model . . . . .	11
2.2 The link transmission model . . . . .	13
<b>3 The two-signal ring road without offset</b>	<b>16</b>
3.1 Apply LTM to boundary flows . . . . .	17
3.2 Stationary states . . . . .	18
3.3 Macroscopic fundamental diagram . . . . .	19
<b>4 The two-signal ring road with offset</b>	<b>23</b>
4.1 Apply LTM to boundary flows . . . . .	24
4.2 Conditions with a green ratio no more than 0.5 . . . . .	25
4.2.1 Derivation of critical densities and MFD . . . . .	25
4.2.2 Capacity of the system . . . . .	30
4.3 Conditions with a green ratio more than 0.5 . . . . .	31
4.3.1 Derivation of critical densities and MFD . . . . .	31
4.3.2 Capacity of the system . . . . .	35
<b>5 Optimal signal settings</b>	<b>40</b>
5.1 Maximum flow-rate for various initial conditions . . . . .	40
5.2 Optimal cycle lengths . . . . .	42

<b>6</b>	<b>Numerical Simulation</b>	<b>47</b>
6.1	Convergency . . . . .	48
6.2	Minimum period . . . . .	50
6.3	MFDs from simulation . . . . .	53
6.4	Relationship between capacity and link length . . . . .	54
<b>7</b>	<b>Summary</b>	<b>56</b>
7.1	Conclusion and findings . . . . .	56
7.2	Future research . . . . .	57
	<b>Bibliography</b>	<b>59</b>

# LIST OF FIGURES

	Page
1.1 Traditional illustration of delay . . . . .	5
2.1 A ring road with N rotationally symmetric signals . . . . .	11
2.2 (a) A ring road with two symmetric signals (b) An infinite one-way street . .	12
2.3 Definitions of link demands and supplies . . . . .	13
3.1 A periodic extension of the spatial-temporal domain without offset . . . . .	17
3.2 MFD of the two-signal ring road without offset . . . . .	22
4.1 A periodic extension of the spatial-temporal domain with offset for green ratio no more than 0.5 . . . . .	25
4.2 MFD of the two-signal ring road with offset (a) . . . . .	29
4.3 Capacity of the two-signal ring road with $\pi \leq 0.5$ . . . . .	30
4.4 MFD of the two-signal ring road with offset (b) . . . . .	31
4.5 A periodic extension of the spatial-temporal domain with offset for green ratio more than 0.5 . . . . .	32
4.6 MFD of the two-signal ring road with offset (c) . . . . .	35
4.7 Capacity of the two-signal ring road with $\pi > 0.5$ . . . . .	38
4.8 MFD of the two-signal ring road with offset (d) . . . . .	39
6.1 Flow chart of $G_a$ and $g_a$ . . . . .	48
6.2 Flow charts of $d_a$ and $s_a$ . . . . .	49
6.3 Convergence of the LTM with respect to total simulation time . . . . .	50
6.4 Convergence of the LTM with respect to time-step size . . . . .	50
6.5 The periods with respect to multiple times of the cycle length (a) . . . . .	51
6.6 The periods with respect to multiple times of the cycle length (b) . . . . .	52
6.7 The periods with respect to multiple times of the cycle length (c) . . . . .	52
6.8 Simulated MFD of the one-signal ring road and the two-signal without offset	54
6.9 Simulated MFD of the two-signal ring road with offset . . . . .	55
6.10 Simulated capacity of the two-signal ring road with offset . . . . .	55
7.1 A ring road with two nonsymmetric signals . . . . .	58

# ACKNOWLEDGMENTS

First, I would like to express my great appreciation to my advisor, Professor Wenlong Jin, for his academic guidance and financial support. He continuously taught me lots of useful knowledge, experience and skills, and patiently led me to think deeply and furtherly about my research. Now, I feel more interested in and motivated for my study. His rigorous academic attitude and concentration on work, encouraged me a lot to devote myself to research.

Secondly, I would like to thank Professor Will Recker and Professor R. Jayakrishnan to be my thesis committee members. They offered me many excellent courses to help me have a better understanding of transportation engineering, and gave me some valuable advice on my research.

Thirdly, I would like to thank Professor Yifeng Yu for his important academic contributions, which provided theoretical support to my thesis, and his helpful suggestions to my research.

Fourthly, I would like to express my gratitude to my friends in UCI and all students in my group, especially Zhe (Jared) Sun, Qinglong Yan and Yue Zhou, for their companion, meaningful discussions and technical assistance.

Last but not least, I would like to thank my family, especially my mother, for their continuous support all these years and encouragement when I felt frustrated.

# ABSTRACT OF THE THESIS

Analysis and design of a stationary ring road with two signals

By

Shizhe Shen

Master of Science in Civil Engineering

University of California, Irvine, 2016

Professor Wenlong Jin, Chair

The signalized ring road is an important model to understand the properties of signal setting on road networks. Stationary states exist on signalized ring road with a minimum period of multiple times of the cycle length. In this study, we extend the homogeneous one-signal ring road to the rotationally symmetric two-signal ring road, and set offsets between signals to reveal coordination effects. First, we apply link transmission model (LTM) to solve boundary flows at signals under stationery states, which is an equilibrium state of the dynamics networks. Then, we derive the critical densities influenced by signal settings, including the cycle length and the green ratio, to determine the conditions for maximum flow-rates of networks. Based on critical densities, an approximate macroscopic fundamental diagram (MFD) is obtained, relating average flow-rate and density of networks. The capacity drop of networks caused by offsets is also analyzed for different ratios of road length and cycle length. We then find the optimal cycle length for various congestion conditions based on the approximate MFD and properties of critical densities. Numerical LTM simulations are run to verify theoretical results and further explore the minimum periods of stationery states.



# Chapter 1

## Introduction

### 1.1 Background

Nowadays, the traffic congestion problem has been increasingly serious, and causes great losses to travelers' time and money. Not only the low efficiency of transportation system is harmful to social benefits, but also emission and noise pollutions lead to environmental problems and endanger public health. In addition, the low capacity of the road networks can waste the society's resources, like more gasoline consumption, and people need to depart earlier for fear of congestion. The continuous congestion condition can also threaten the road safety condition, especially the stop-and-go state will increase the rate of accidents because drivers cannot react to change of the traffic state in time when they are tired or in bad mood.

Consequently, it is necessary to increase the road networks' capacities so as to improve the operation efficiency. However, for most cities, it is impossible to expand the roads in large scale due to the space limitation on construction along the road and constraints of budget. Besides, increasing the road networks' capacity simply by roads expansion will only attract more vehicles and further worsen the congestion condition. Therefore, the scientific methods

to increase the networks' capacity should be based on the system optimization.

Among all the components of the road networks, especially among traffic control strategies, the traffic signal is the most influential factor to traffic performance, and we can change the signal settings with a relatively low cost. A good regional signal plan can improve the capacity of the road network and relieve congestion problem in a very short time. Developing an appropriate signal design method to optimize the efficiency of the whole network system is quite significant and necessary.

## **1.2 Traditional methods for signal design**

Traditionally, we study the signal design for each intersection individually based on volumes of all directions with several critical assumptions. In [15], there are detailed introductions to traditional signal design methods for both pre-timed and actuated signals. Delay is seen as the most important measure of effectiveness, utilized to the analysis of the signal plan. Apart from the design for the individual intersection, signal-coordination is applied to improve the capacity the network.

### **1.2.1 Cycle length**

There are three classical signal operation types, pre-timed, semi-actuated and full actuated. For the pre-timed signal operation, the cycle length, phase sequence, and timing of each interval are constant, of course we need to set a optimal cycle length. For the semi-actuated operation, we only set detectors on the minor approaches, while for the full actuated operation, we need to set detectors on every lane of each approach. Even though the cycle length is not constant, we also need to find the critical cycle. Traditionally, we find an appropriate cycle length by minimizing the average per vehicle delay, which means we should make the

cycle length as short as possible. Ideally, the best cycle setting is that in each cycle, one phase is allocated the time to release only one vehicle. However, the demand cannot be satisfied if the cycle length is too short due to the lost time. The total lost time consists of the start-up loss and the clearance loss. The start-up loss happens because the headways for the first several vehicles to leave in each cycle are much larger than the saturation headway due to the drivers' reaction time and acceleration of vehicles. The clearance loss happens at the end of the green time, it is hard to observe and is defined as the time interval between the last vehicles front wheels crossing the stop line and the initial of the green time for the next phase. So the actually used green time doesn't equal the actual green time. The effective green time can be seen as the actually used green time, and can be stated as the amount of time when vehicles can actually move:

$$g_i = G_i + Y_i - t_{Li}$$

where:

$g_i$  = effective green time for movement(s) i,

$G_i$  = actual green time for movement(s) i,

$Y_i$  = sum of yellow and all red intervals for movement(s) i,

$t_{Li}$  = total lost time (sum of start-up loss and clearance loss) for movement(s) i.

The minimum acceptable cycle length should be just enough to satisfy the demand of a specific volume condition so that the vehicles' average delay can be reduced to the minimum.

The formula is as follows:

$$C_{\min} = \frac{N * t_L}{1 - (\frac{V_C}{3600/h})}$$

where:

$N$ : number of phases in the cycle,

$t_L$  = total lost time, s

$V_C$ : maximum sum of critical-lane volumes, veh/h

$h$ : saturation headway, s/veh

### 1.2.2 Delay

The common measures to assess the intersection operational qualities are delay, queue and stops. Among the measures, delay is the most common and significant. Traditionally, the analytical models are based on several assumptions, (1) the arrival rate is uniform, (2) the queue is building at a point location. Without preexisting queue, we can get the classic arrival and departure pattern, in Figure 1.1. Analytical models usually consists of three components, uniform delay, random delay and overflow delay. Random delay is the supplement to uniform delay while overflow delay occurs when demand surpasses capacity.

The Webster's uniform delay model is the start and base of the analytical model. The aggregated delay is the area of the triangle enclosed by the arrival and departure curve. So the average delay is as follows:

$$UD = \frac{1}{2}C \frac{(1 - \frac{g}{C})^2}{1 - \frac{v}{s}}$$

where:

$UD$ : average uniform delay per vehicle, s

$C$ : cycle length, s

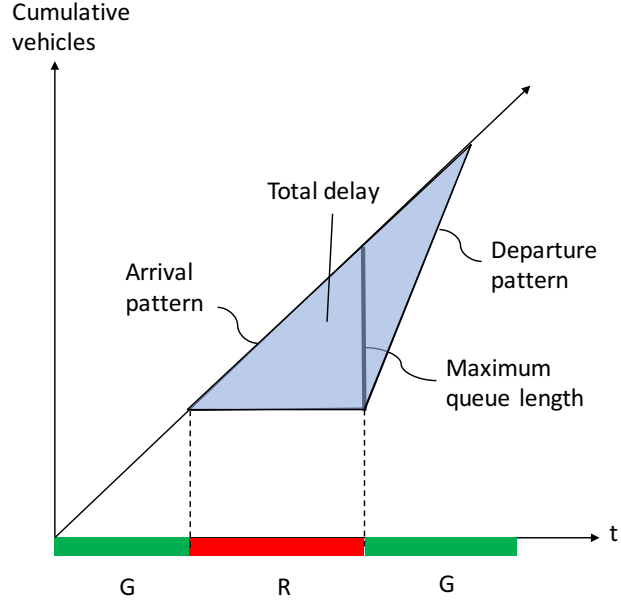


Figure 1.1: Traditional illustration of delay

$g$ : effective green time, s

$v$ : arrival flow-rate, veh/h

$s$ : saturation flow rate, veh/h

However, the arrival rate cannot be uniformly distributed in reality, so the model need to add a random term to make the arrival rate stochastic, by assuming that inter-vehicle arrival times are Poisson distributed. The most common random delay model, Webster formulation, is as follos:

$$RD = \frac{X^2}{2v(1 - X)}$$

where:

$RD$ : average random delay per vehicle, s

$X$ :  $v/c$  ratio, ( $c$  is the capacity of the approach, veh/h )

The terms above are based on the assumption that the demand does not exceed the capacity so that at the beginning of every cycle, there will be no vehicle waiting in the queue. However, when the over-saturation happens, which means the arrival rate exceeds the capacity, a new term is necessary for the overflow delay. If at the beginning ( $t=0$ ), there is no vehicle in the queue, during the time period from  $T_1$  to  $T_2$ , the average overflow delay is:

$$OD = \frac{T_1 + T_2}{2}(X - 1)$$

where:

$OD$ : average overflow delay per vehicle, s

### 1.2.3 Signal coordination

When signals are close to each other, vehicles may have to stop frequently, even to stop in every intersection, without the coordination between each intersection. Idle time and the start-up loss will take up a large proportion of the total travel time. For an arterial with high flow-rate, flow-rates on the intersected roads are usually much lower. If we can optimize the signal settings to reduce the stop times on the arterial, the operation efficiency of road networks can be improved significantly.

For an arterial with the application of signal coordinations, the cycle lengths of all the intersections must be the same or integral multiple of others' to ensure the coordination system is stable. The difference of initial green time between two consecutive intersections is called the offset. Usually, for signal progressions on one-way streets, the ideal offset is obtained from the following:

$$t_{ideal} = \frac{L}{S}$$

where:

$t_{ideal}$ : ideal offset, s

$L$ : distance between consecutive intersections, ft

$S$ : vehicle speed, ft/s

In the state-of-the-practice, we also need to subtract the start-up loss time for the first coordinated intersection. In addition, if there are queues at the beginning of the green time, caused by vehicles from the turning movement streams or other origins between the intersections, they may affect the arriving platoons from upstreams, so we also need to adjust the ideal offset by subtracting the time for the queue to dissipate:

$$t_{adj} = \frac{L}{S} - (Qh + l_1)$$

where:

$t_{adj}$ : adjusted ideal offset, s

$Q$ : number of vehicles queued per lane, veh

$h$ : discharge headway of queued vehicles, s/veh

$l_1$ : start-up lost time, s

For each intersection, even though the cycle lengths are the same, the green times are different, so the time for vehicles to pass through several intersections continuously can vary a lot. Sometimes influenced by other practical factors, like the drop of the platoon speed, the time can be very small. So we need a new concept, bandwidth, to represent the amount of green time that can be used by a platoon passing through all the coordinated intersections. Bandwidth is defined as the time difference between the first and the last vehicle that can

pass through the entire system without stopping. Two common measures of bandwidth are the efficiency and the capacity. The efficiency of the bandwidth is the ratio of the bandwidth to the cycle length:

$$EFF_{BW} = (\frac{BW}{C}) * 100\%$$

where:

$EFF_{BW}$ : bandwidth efficiency

$BW$ : bandwidth, s

$C$ : Cycle length, s

The capacity of the bandwidth is the number of vehicles in one platoon which can pass through the system without stopping:

$$c_{BW} = \frac{3600 * BW * NL}{C * h}$$

where:

$c_{BW}$ : bandwidth capacity, veh/h

$NL$ : number of through lanes

$h$ : saturation headway, s

### 1.3 New methods for signal design

Although the traditional signal design methods are rational to some extent, especially in practice, and widely applied, however, the aforementioned assumptions on which these meth-



ods based are not reasonable. In [11], it was pointed out the limitations of the Webster's delay formula. In addition, these methods cannot capture the traffic wave on the link and other traffic phenomenons, like queue spillbacks, so they are actually helpless at the analysis stage. Considering the deficiencies above, [11] developed a new method to study the signal design based on the traffic flow theory by building a signalized ring road, and maximize the average flow-rate by optimizing signal settings in stationary states. [9] proved the existence of the stationary solutions for the kinematic wave model on networks with an invariant junction model, and origin demands, destination supplies and route choice proportions are constant. In [10], the asymptotical convergency pattern on the signalized ring road and the feature of the system period was proven mathematically, which certifies the existence of stationery states on signalized ring roads. The theoretical work is a solid foundation to the further study.

The link transmission model ([16]) was applied to the signalized ring road to analyze the dynamic patterns. In [8], the Newell's simplified kinematic wave model ([13]) was proven by the Hopf-Lax formula ([5]) on the LWR model ([12]; [14]), and two continuous formulations of link transmission model were derived based on the definition of link demand and supply ([1]).

The macroscopic fundamental diagram (MFD) of one street or even a region reveals the relationship between the average flow-rate and density ([7]). [6] verified the existence of MFD on networks by real data. In [4], the capacity of the street with no turns was derived by variational theory ([2]; [3]), and the approximate MFD of the street was obtained by various practical cuts.

# Chapter 2

## Problem statement

To eliminate the limitations of traditional signal design methods and analyze the signal problem systematically, in [11], a one-signal ring road was built, which is equivalent to a simple network composed of infinite one-way streets without turning movements, and all links, including traffic conditions on the links, and signal settings of all signals are the same. MFDs with different initial conditions and signal settings are then derived, and based on MFD, the optimal cycle length can be attained with the lost time on each phase. However, we can't consider the effects of offsets between consecutive intersections, so we need to extend the one-signal ring road to a ring road with  $N$  rotationally symmetric signals and links (Figure 2.1), with all links identical and homogeneous, cycle lengths  $T$  and green ratios  $\pi$  of all signals are the same. Moreover, the initial conditions indicated by the average density  $k_0$  of each link are the same. Then we can set offsets on the network, the offset  $\delta$ , between consecutive signals, is  $\frac{T}{N}$  so as to ensure that signal settings and locations of signals are both rotationally symmetrically distributed.

Similar to the one-signal ring road, we can derive MFD of the network for various situations:

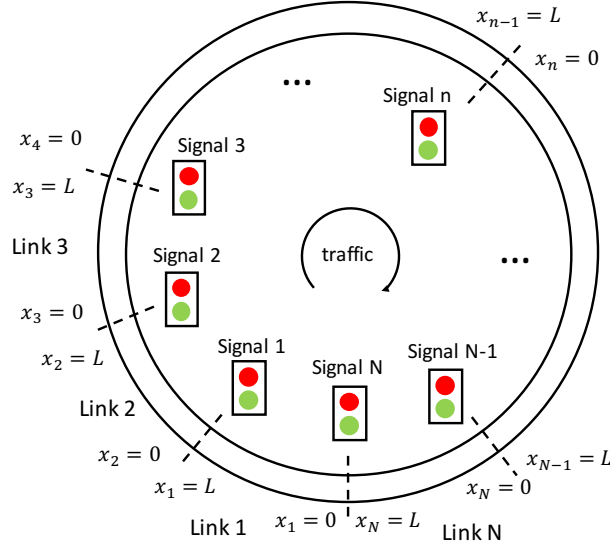


Figure 2.1: A ring road with  $N$  rotationally symmetric signals

$$\bar{q} = \bar{Q}(k_0; T, \pi, \delta). \quad (2.1)$$

In addition, we can also find the best cycle length  $T$  and offset  $\delta$  by considering the lost time to maximize  $\bar{Q}(k_0; T, \pi, \delta)$  for various initial conditions.

## 2.1 The LWR model

First, we should start with the two-signal ring road model, which is the simplest case and a significant process from the one-signal ring road to the  $N$ -signal ring road. Extend the original ring road model with one signal to a ring road with two symmetrical signals, which divide the the ring road into two roads (Figure 2.2a), the left side is Link 1 while the right side is Link 2, the signal above is Signal 1 while the signal below is Signal 2. The length of the ring road is  $2L$ , and the length of each link is  $L$ .

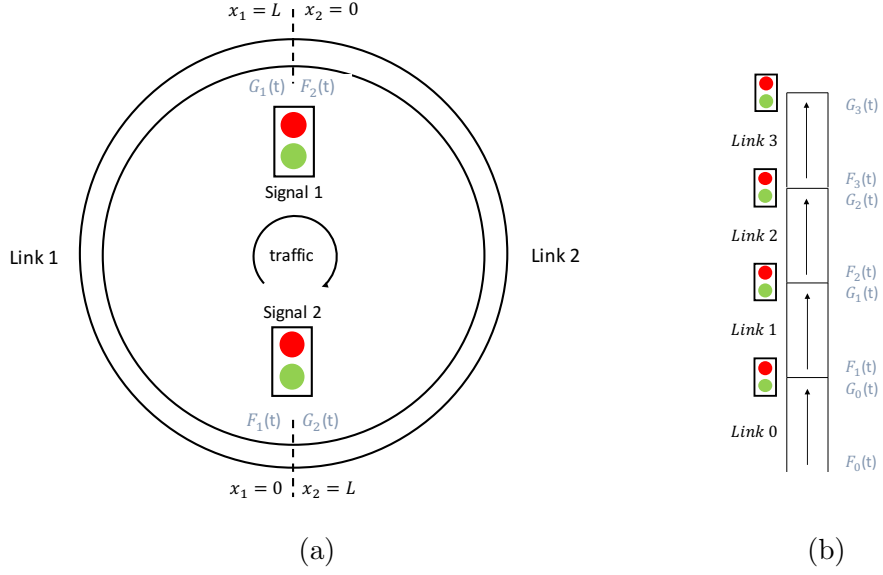


Figure 2.2: (a) A ring road with two symmetric signals (b) An infinite one-way street

The movement rule of the ring road model is based on the LWR model:

$$\frac{\partial k_a}{\partial t} + \frac{\partial B(x_a, t) Q(k_a)}{\partial x} = 0 \quad (2.2)$$

where  $k_a(x_a, t)$  is the traffic density on Link  $a$  ( $a \in \mathbb{Z}$ ), and  $x_a \in [0, L]$ .

$B(x_a, t)$  is the equation representing the signal effects,  $B(x_a, t) = 1 - I(x_a) \cdot (1 - \beta_a(t))$ .  $I(x_a)$  is the location parameter for signals,

$$I(x_a) = \begin{cases} 1 & x_a = 0, L \\ 0 & \text{otherwise} \end{cases}$$

$\beta_a(t)$  is the time parameter of Signal  $a$ , depending on when the signal is green and when the signal is red, so it is related to the offset setting. We will define  $\beta_1(t)$  and  $\beta_2(t)$  later.

The fundamental diagram utilized is a triangular fundamental diagram:

$$Q(k) = \min\{Vk, (K - k)W\}, \quad (2.3)$$

where  $V$  is the free-flow speed,  $-W$  is the shock wave speed, and  $K$  is the jam density. The critical density corresponding to the capacity  $C$  is  $\bar{K} = \frac{W}{V+W}K = \frac{C}{V} = K - \frac{C}{W}$ .

## 2.2 The link transmission model

In [8], continuous formulas for a link's demand and supply were derived for the link transmission model (Figure 2.3), and we can apply LTM demand and supply functions to the ring road with two symmetrical signals. The initial condition on Link  $a$  is denoted by  $N_a(x_a)$ , and the average densities of both links are  $k_0$  initially. The boundary conditions of Link  $a$  are  $G_a(t)$  (accumulative out-flow) and  $F_a(t)$  (accumulative in-flow), respectively, and we have  $F_a(0) = G_a(0) + k_0L$ .

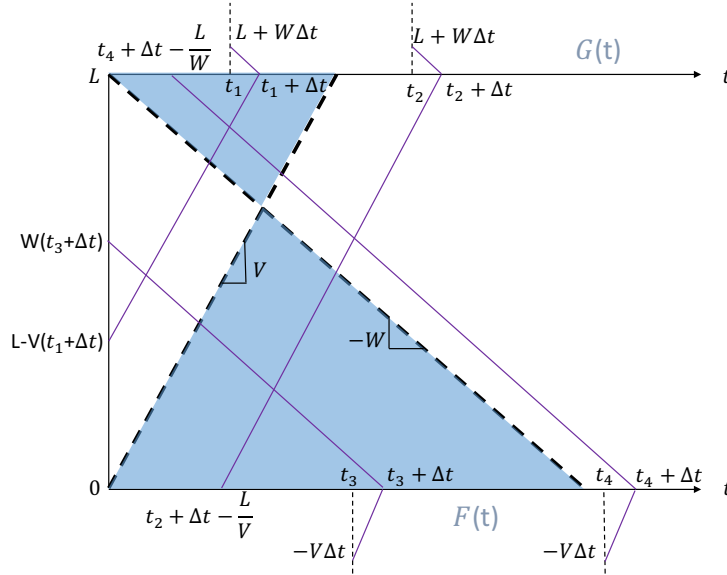


Figure 2.3: Definitions of link demands and supplies

The corresponding flow-rates of Link  $a$  are  $g_a(t) = \frac{dG_a(t)}{dt}$  and  $f_a(t) = \frac{dF_a(t)}{dt}$ , and  $f_a(t) = g_{a-1}(t)$ . We set  $G_a(0) = G_{a-1}(0)$  for any  $a$ , so  $F_a(0) = G_{a-1}(0) + k_0L$ . Then for any  $t$ ,  $F_a(t) = F_a(0) + \int_0^t f_a(t)dt = G_{a-1}(0) + k_0L + \int_0^t g_{a-1}(t)dt = G_{a-1}(t) + k_0L$ .

Boundary conditions are repeated, which means the upstream and downstream links of Link  $a$  are the same (Figure 2.2b), then we have  $G_a(t) = G_{a-2}(t)$ ,  $F_a(t) = F_{a-2}(t)$  and  $\beta_a(t) = \beta_{a-2}(t)$  for any  $a$  and  $t$ , so that the ring road can be extended as a network, consisting of the same links, as in Figures 3.1, 4.1, and 4.5.

In [11], the cumulative flow  $A(x, t)$  was used for each boundary flow and the x-axis of the whole network is continuous, while in this study, boundary flows of every two adjacent links are repeated and the x-axes for each link are independent.

Initially, if vehicles are evenly distributed on the link, and  $G_a(0) = 0$  for any  $a$ , so  $N(x_a) = k_0 x_a$ ,  $F_a(0) = G_{a-1}(0) + k_0 L = k_0 L$ . The demand and supply functions for Link  $a$  are

$$d_a(t) = \begin{cases} \min \{k_0 V + H(\lambda_a(t)), C\}, & t \leq \frac{L}{V} \\ \min \{g_{a-1}(t - \frac{L}{V}) + H(\lambda_a(t)), C\}, & t > \frac{L}{V} \end{cases} \quad (2.4a)$$

$$s_a(t) = \begin{cases} \min \{(K - k_0)W + H(\gamma_a(t)), C\}, & t \leq \frac{L}{W} \\ \min \{g_a(t - \frac{L}{W}) + H(\gamma_a(t)), C\}, & t > \frac{L}{W} \end{cases} \quad (2.4b)$$

where the link queue size  $\lambda_a(t)$  and vacancy size  $\gamma_a(t)$  are

$$\lambda_a(t) = \begin{cases} k_0 V t - G_a(t), & t \leq \frac{L}{V} \\ G_{a-1}(t - \frac{L}{V}) - G_a(t) + k_0 L, & t > \frac{L}{V} \end{cases} \quad (2.4c)$$

$$\gamma_a(t) = \begin{cases} (K - k_0)W t - G_{a-1}(t), & t \leq \frac{L}{W} \\ G_a(t - \frac{L}{W}) + (K - k_0)L - G_{a-1}(t), & t > \frac{L}{W} \end{cases} \quad (2.4d)$$

$H(z)$  is the indicator function for  $z \geq 0$ ,

$$H(z) = \lim_{\Delta t \rightarrow 0^+} \frac{z}{\Delta t} = \begin{cases} 0 & z = 0 \\ +\infty & z > 0 \end{cases}$$

The boundary flow-rate at Signal  $a$  is decided by signal settings, the demand of the upstream link and the supply of the downstream link ([1]):

$$g_a(t) = \beta_a(t) \min \{d_a(t), s_{a-1}(t)\}. \quad (2.5)$$

# Chapter 3

## The two-signal ring road without offset

The two-signal Ring road without offset can actually be seen as the double extension of the original signalized ring road model, because the new added link and signal are only the duplication of the original ones. The two links share the same road characteristics, the same signal settings of both upstream and downstream signals, and the same initial condition, so during the running process, the distribution patterns of the two links and boundary flow-rates for two signals at a specific time are exactly the same. The extension of the spatial-temporal domain for the network is also the same as the previous one-signal model (Figure 3.1). Therefore, without any additional derivations, we can believe that for one initial condition and signal setting, both MFDs should be completely overlapped, and we can see it from simulation results. However, to make sure that the judgement is correct, we can prove it by LTM, and without offset,  $\beta_1(t)$  and  $\beta_2(t)$  are the same.

$$\beta_1(t) = \beta_2(t) = \begin{cases} 1, & t - iT \in [0, \pi T], i = 1, 2, \dots \\ 0, & \text{otherwise} \end{cases} \quad (3.1)$$



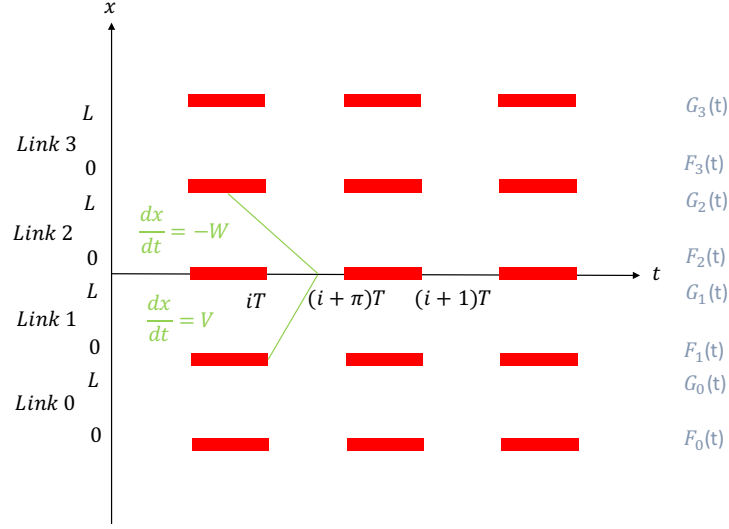


Figure 3.1: A periodic extension of the spatial-temporal domain without offset

### 3.1 Apply LTM to boundary flows

In [11], the equations for the boundary flow of the signalized ring road are derived from the continuous LTM at a large time  $t$ , we can apply it to the two-signal ring road, equations for boundary flows are as follows:

$$G_1(t) = \min\{G_2(t - \frac{L}{V}) + k_0L, G_2(t - \frac{L}{W}) + (K - k_0)L, G_1(iT) + (t - iT)C\}, \quad (3.2a)$$

for  $t - iT \in (0, \pi T]$ , which is green time, and

$$G_1(t) = G_1((i + \pi)T), \quad (3.2b)$$

for  $t - iT \in (\pi T, T]$ , which is red time.

$$G_2(t) = \min\{G_1(t - \frac{L}{V}) + k_0 L, G_1(t - \frac{L}{W}) + (K - k_0)L, G_2(iT) + (t - iT)C\}, \quad (3.3a)$$

for  $t - iT \in (0, \pi T]$ , which is green time, and

$$G_2(t) = G_2((i + \pi)T), \quad (3.3b)$$

for  $t - iT \in (\pi T, T]$ , which is red time.

The formulas show that during the green time, there are three characteristic waves that can affect the boundary flows, the forward wave with the free-flow speed  $V$ , the backward wave with the shock wave speed  $-W$ , and the stationary wave at the boundaries.

## 3.2 Stationary states

In [10], the asymptotic convergency pattern of the signalized ring road was proven mathematically. After a long time, the system can reach a periodical steady state with a constant period, which was called the stationary state in [11]. So during a period, the average flow-rate at any point is equal to the system's average flow-rate, which means  $\bar{g}_1 = \bar{g}_2 = \bar{g}$ , where  $\bar{g}_1$ ,  $\bar{g}_2$  and  $\bar{g}$  are the average flow-rates of two boundaries and the system during a period. If  $\bar{g}_1 \neq \bar{g}_2$ , like  $\bar{g}_1 > \bar{g}_2$ , then during every period, more vehicles enter Link 2 than those leave, and more vehicles leave Link 1 than those enter, as time goes on, all vehicles remain in Link 2, it is not reasonable, so the stationary state ([11]) also exists in the two-signal ring road model.

In [10], it was also proven that the minimum period is  $mT$ , an integer multiple of the cycle length, and when  $\bar{g}$  reaches the capacity  $\pi C$ , or the cycle length  $T$  is large,  $m = 1$ .

Considering that  $m$  can be very large on some conditions, we assume that the period is the cycle length  $T$  for analysis, even when  $T$  is relatively small and  $\bar{g} < \pi C$ . So  $g_a(t+T) = g_a(t)$  when  $t$  is large, then we can define the periodical flow patterns as follows:

$$G_a(t+T) = G_a(t) + \bar{g}_a T, \quad (3.4)$$

where  $\bar{g}_a$  is the average flow-rate at the Signal  $a$  during a cycle, and  $\bar{g}_a \in [0, \pi C]$ .

### 3.3 Macroscopic fundamental diagram

First, we divide the free-flow travel time  $\frac{L}{V}$  and the shock wave propagation time  $\frac{L}{W}$  by the cycle length  $T$ , respectively,  $j_1$  and  $j_2$  are moduli while  $\alpha_1$  and  $\alpha_2$  are reminders:

$$\frac{L}{V} = \theta_1 T = (j_1 + \alpha_1)T, \quad j_1 = \lfloor \frac{L}{VT} \rfloor = 0, 1, \dots, \quad 0 \leq \alpha_1 < 1, \quad (3.5a)$$

$$\frac{L}{W} = \theta_2 T = (j_2 + \alpha_2)T, \quad j_2 = \lfloor \frac{L}{WT} \rfloor = 0, 1, \dots, \quad 0 \leq \alpha_2 < 1, \quad (3.5b)$$

where  $\lfloor \cdot \rfloor$  is the floor function.

Then, we can define two critical densities,  $k_1$  and  $k_2$ :

$$k_1 = \frac{j_1 + \min\{\frac{\alpha_1}{\pi}, 1\}}{j_1 + \alpha_1} \pi \bar{K}, \quad (3.6a)$$

$$k_2 = K - \frac{j_2 + \min\{\frac{\alpha_2}{\pi}, 1\}}{j_2 + \alpha_2} \pi (K - \bar{K}). \quad (3.6b)$$

When  $k_1 \leq k_0 \leq k_2$ , the average system flow-rate  $\bar{g}$  is  $\pi C$ .

*Proof.* According to (3.2a), at the end of the green time for each signal, the boundary flows

can be represented as

$$\begin{aligned} G_1(iT + \pi T) &= \min\{G_2((i - j_1 + \pi - \alpha_1)T) + k_0L, G_2((i - j_2 + \pi - \alpha_2)T) \\ &+ (K - k_0)L, G_1(iT) + \pi TC)\} = G_1(iT) + \bar{g}_1T, \end{aligned} \quad (3.7a)$$

and

$$\begin{aligned} G_2(iT + \pi T) &= \min\{G_1((i - j_1 + \pi - \alpha_1)T) + k_0L, G_1(i - j_2 + \pi - \alpha_2)T) \\ &+ (K - k_0)L, G_2(iT + \pi TC)\} = G_2(iT) + \bar{g}_2T. \end{aligned} \quad (3.7b)$$

$\bar{g} = \bar{g}_1 = \bar{g}_2 = \pi C$  can happen only when during the green time of each signal,  $g_1(t) = C$  and  $g_2(t) = C$  are always satisfied, so we have  $\bar{g} = \pi C$  if and only if

$$\begin{aligned} G_2((i - j_1 + \pi - \alpha_1)T) + k_0L &\geq G_1(iT) + \pi TC, \\ G_1((i - j_1 + \pi - \alpha_1)T) + k_0L &\geq G_2(iT) + \pi TC, \end{aligned} \quad (3.8a)$$

and

$$\begin{aligned} G_2((i - j_2 + \pi - \alpha_2)T) + (K - k_0)L &\geq G_1(iT) + \pi TC, \\ G_1((i - j_2 + \pi - \alpha_2)T) + (K - k_0)L &\geq G_2(iT) + \pi TC. \end{aligned} \quad (3.8b)$$

For the first equation group, we have the following two scenarios:

(1) If  $\alpha_1 > \pi$ ,  $2k_0L \geq (G_1(iT) - G_1((i - j_1 + \pi - \alpha_1)T)) + (G_2(iT) - G_2((i - j_1 + \pi - \alpha_1)T)) + 2\pi TC = j_1\bar{g}_1T + j_1\bar{g}_2T + 2\pi TC = 2j_1\bar{g}T + 2\pi TC$ . Thus  $k_0 \geq \frac{(j_1+1)\pi C}{(j_1+\alpha_1)V}$ .

(2) If  $\alpha_1 \leq \pi$ ,  $2k_0L \geq (G_1(iT) - G_1((i - j_1 + \pi - \alpha_1)T)) + (G_2(iT) - G_2((i - j_1 + \pi - \alpha_1)T)) + 2\pi TC = (j_1 + \frac{\alpha_1}{\pi})\bar{g}_1T + (j_1 + \frac{\alpha_1}{\pi})\bar{g}_2T + 2\pi TC = (2j_1 + \frac{2\alpha_1}{\pi})\bar{g}T + 2\pi TC$ . Thus  $k_0 \geq \frac{(j_1+\frac{\alpha_1}{\pi})\pi C}{(j_1+\alpha_1)V}$ .

Above is for necessary condition, and the following is for sufficient condition:

Since  $\bar{g}_1 = \bar{g}_2$ , and in (3.2a) and (3.3a), the first term  $G_a(t - \frac{L}{V}) + k_0L$  corresponds to a

small  $k_0$ , while the second term  $G_a(t - \frac{L}{W}) + (K - k_0)L$  corresponds to a large  $k_0$ . Then for a small  $k_0$ ,  $G_1((i - j_1 + \pi - \alpha_1)T) + k_0L < G_2(iT) + \pi TC$  and  $G_2((i - j_1 + \pi - \alpha_1)T) + k_0L < G_1(iT) + \pi TC$  are both met, while for a large  $k_0$ ,  $G_2((i - j_1 + \pi - \alpha_1)T) + k_0L \geq G_1(iT) + \pi TC$  and  $G_1((i - j_1 + \pi - \alpha_1)T) + k_0L \geq G_2(iT) + \pi TC$  are both met. So  $G_2((i - j_1 + \pi - \alpha_1)T) + k_0L \geq G_1(iT) + \pi TC$  and  $G_1((i - j_1 + \pi - \alpha_1)T) + k_0L < G_2(iT) + \pi TC$ , or  $G_2((i - j_1 + \pi - \alpha_1)T) + k_0L < G_1(iT) + \pi TC$  and  $G_1((i - j_1 + \pi - \alpha_1)T) + k_0L \geq G_2(iT) + \pi TC$  are not possible.

In summary, the first equation group (3.8a) is equivalent to  $k_0 \geq k_1$ . Similarly, we can prove that the second equation group (3.8b) is equivalent to  $k_0 \leq k_2$ .  $\square$

We can find that the two new critical densities are exactly the same as the critical densities in [11] for the one-signal ring road, so we also have the following relationship:

$$\pi \bar{K} \leq k_1 \leq \bar{K} \leq k_2 \leq K - \pi(K - \bar{K}). \quad (3.9)$$

When  $k_0 < k_1$ ,  $G_2((i - j_1 + \pi - \alpha_1)T) + k_0L < G_1(iT) + \pi TC$  and  $G_1((i - j_1 + \pi - \alpha_1)T) + k_0L < G_2(iT) + \pi TC$ , so we have

$$G_1(iT) + \bar{g}T = G_2((i - j_1 + \pi - \alpha_1)T) + k_0L,$$

$$G_2(iT) + \bar{g}T = G_1((i - j_1 + \pi - \alpha_1)T) + k_0L.$$

When  $\alpha_1 \geq \pi$ ,  $\bar{g} = \frac{2k_0L}{2(j_1+1)T} = \frac{k_0}{k_1}\pi C$ .

When  $\alpha_1 \geq \pi$ , we assume that when  $\bar{g} < \pi C$ ,  $g(t)$  is also evenly distributed during the green time,  $\bar{g} = \frac{2k_0L}{2(j_1+\frac{\alpha_1}{\pi})T} = \frac{k_0}{k_1}\pi C$ .

So,  $\bar{g} \approx \frac{k_0}{k_1}\pi C$ . Similarly, when  $k_0 > k_2$ ,  $\bar{g} \approx \frac{K-k_0}{K-k_1}\pi C$ .

We can get the same trapezoidal or triangular MFD as the one-signal ring road ([11]):

$$\bar{g}(k_0; T, \pi) \approx \begin{cases} \Phi_1(k_0; T, \pi), & 0 \leq k_0 < k_1 \\ \pi C, & k_1 \leq k_0 \leq k_2 \\ \Phi_2(k_0; T, \pi), & k_2 < k_0 \leq K \end{cases} = \begin{cases} \frac{k_0}{k_1} \pi C, & 0 \leq k_0 < k_1 \\ \pi C, & k_1 \leq k_0 \leq k_2 \\ \frac{K-k_0}{K-k_1} \pi C, & k_2 < k_0 \leq K \end{cases} \quad (3.10)$$

The shape of MFD is shown by the thick blue lines of Figure 3.2, and the thin black solid lines are boundaries for MFD.

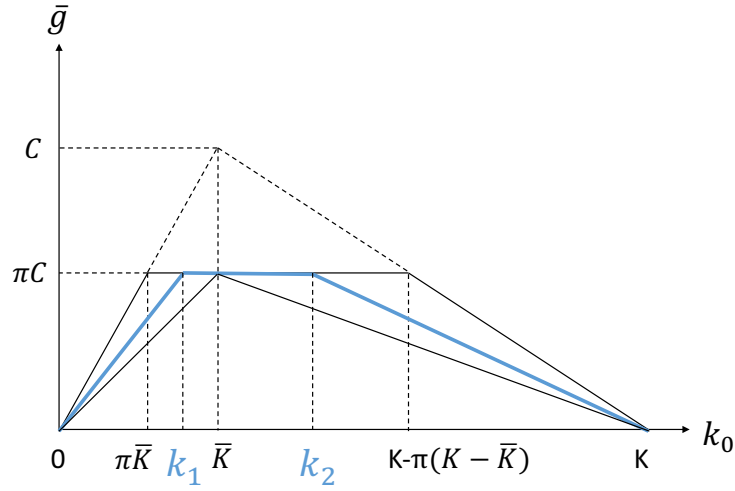


Figure 3.2: MFD of the two-signal ring road without offset

# Chapter 4

## The two-signal ring road with offset

For the two-signal ring road with offset, to make signal settings and offset patterns for two adjacent links of the extended network symmetric, we can start with setting the offset as  $\frac{T}{2}$ , so the offset from Signal 1 to Signal 2, and that from Signal 2 to Signal 1 are both  $\frac{T}{2}$ . Extensions of the spatial-temporal domain for the network are in Figures 4.1 (green ratio  $\pi \leq 0.5$ ) and 4.5 (green ratio  $\pi > 0.5$ ).  $\beta_1(t)$  and  $\beta_2(t)$  are defined as follows:

$$\beta_1(t) = \begin{cases} 1, & t - iT \in [0, \pi T], i = 1, 2, \dots \\ 0, & \text{otherwise} \end{cases} \quad (4.1a)$$

$$\beta_2(t) = \begin{cases} 1, & t - iT \in [\frac{T}{2}, \frac{T}{2} + \pi T], i = 1, 2, \dots \\ 0, & \text{otherwise} \end{cases} \quad (4.1b)$$

## 4.1 Apply LTM to boundary flows

First, We apply LTM to the two-signal ring road with offset =  $\frac{T}{2}$ , equations for two boundary flows are as follows:

$$G_1(t) = \min\{G_2(t - \frac{L}{V}) + k_0L, G_2(t - \frac{L}{W}) + (K - k_0)L, G_1(iT) + (t - iT)C\}, \quad (4.2a)$$

for  $t - iT \in (0, \pi T]$ , which is green time, and

$$G_1(t) = G_1((i + \pi)T), \quad (4.2b)$$

for  $t - iT \in (\pi T, T]$ , which is red time.

$$\begin{aligned} G_2(t) = \min\{G_1(t - \frac{L}{V}) + k_0L, G_1(t - \frac{L}{W}) + (K - k_0)L, \\ G_2(iT + \frac{T}{2}) + (t - iT - \frac{T}{2})C\}, \end{aligned} \quad (4.3a)$$

for  $t - iT \in (\frac{T}{2}, \frac{T}{2} + \pi T]$ , which is green time, and

$$G_2(t) = G_2((i + \pi + \frac{1}{2})T), \quad (4.3b)$$

for  $t - iT \in (\frac{T}{2} + \pi T, \frac{3T}{2}]$ , which is red time.

The formula of  $G_1(t)$  is the same as the previous chapter while the formula of  $G_2(t)$  is different because the start of the green time of Signal 2 is  $\frac{T}{2}$  late.

Similarly, we assume that the period is the cycle length  $T$  in stationary states, and from the analysis of the previous chapter, we know that when  $\bar{g} = \pi C$ , during the green time,  $g_1(t) = C$  and  $g_2(t) = C$ , so the flow patterns in each cycle are exactly the same, which means  $m = 1$ . We can say that when  $k_1 \leq k_0 \leq k_2$ , MFD is accurate. Then we have



$g_a(t + T) = g_a(t)$  for any large  $t$ , and the periodical flow patterns are the same as (3.4).

## 4.2 Conditions with a green ratio no more than 0.5

### 4.2.1 Derivation of critical densities and MFD

First, we focus on the conditions when  $\pi \leq 0.5$ , and we need to redefine the critical densities,  $k_1$  and  $k_2$ :

$$k_1 = \frac{j_1 + \max\{\frac{\alpha_1 - \frac{1}{2}}{\pi}, 0\} + \frac{1}{2}\pi\overline{K}}{j_1 + \alpha_1}, \quad (4.4a)$$

$$k_2 = K - \frac{j_2 + \max\{\frac{\alpha_2 - \frac{1}{2}}{\pi}, 0\} + \frac{1}{2}\pi(K - \bar{K})}{j_2 + \alpha_2}. \quad (4.4b)$$

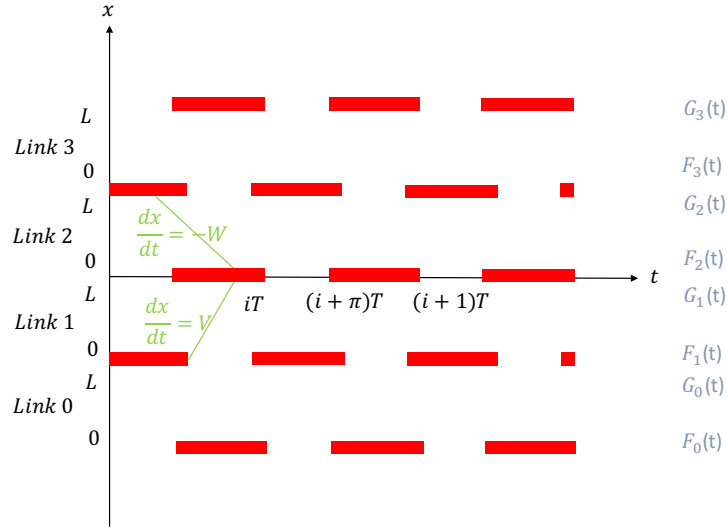


Figure 4.1: A periodic extension of the spatial-temporal domain with offset for green ratio no more than 0.5

**Theorem 4.1.** *In stationary states, when  $k_1 \leq k_0 \leq k_2$ , the system average flow-rate*

$$\bar{g} = \pi C.$$

*Proof.* According to (4.2a) and (4.3a), at the end of the green time of each signal, the boundary flows can be represented as

$$\begin{aligned} G_1(iT + \pi T) &= \min\{G_2((i - j_1 + \pi - \alpha_1)T) + k_0L, G_2((i - j_2 + \pi - \alpha_2)T) \\ &\quad + (K - k_0)L, G_1(iT) + \pi TC\} = G_1(iT) + \bar{g}_1T, \end{aligned} \quad (4.5a)$$

and

$$\begin{aligned} G_2(iT + \frac{1}{2}T + \pi T) &= \min\{G_1((i - j_1 + \frac{1}{2} + \pi - \alpha_1)T) + k_0L, \\ G_1(i - j_2 + \frac{1}{2} + \pi - \alpha_2)T) + (K - k_0)L, G_2(iT + \frac{T}{2}) + \pi TC\} \\ &= G_2(iT + \frac{1}{2}T) + \bar{g}_2T. \end{aligned} \quad (4.5b)$$

So  $\bar{g}_1 = \bar{g}_2 = \bar{g} = \pi C$  if and only if

$$\begin{aligned} G_2((i - j_1 + \pi - \alpha_1)T) + k_0L &\geq G_1(iT) + \pi TC, \\ G_1((i - j_1 + \frac{1}{2} + \pi - \alpha_1)T) + k_0L &\geq G_2(iT + \frac{T}{2}) + \pi TC, \end{aligned} \quad (4.6a)$$

and

$$\begin{aligned} G_2((i - j_2 + \pi - \alpha_2)T) + (K - k_0)L &\geq G_1(iT) + \pi TC, \\ G_1((i - j_2 + \frac{1}{2} + \pi - \alpha_2)T) + (K - k_0)L &\geq G_2(iT + \frac{T}{2}) + \pi TC. \end{aligned} \quad (4.6b)$$

For the first equation group, we have the following two scenarios:

(1) If  $\alpha_1 \leq \frac{1}{2}$ ,  $2k_0L \geq (G_1(iT) - G_1((i - j_1 + \frac{1}{2} + \pi - \alpha_1)T)) + (G_2(iT + \frac{T}{2}) - G_2((i - j_1 + \pi - \alpha_1)T)) + 2\pi TC = (j_1 - 1)\bar{g}_1T + j_1\bar{g}_2T + 2\pi TC = (2j_1 - 1)\bar{g}T + 2\pi TC$ . Thus  $k_0 \geq \frac{(j_1 + \frac{1}{2})\pi C}{(j_1 + \alpha_1)V} = \frac{j_1 + \frac{1}{2}}{j_1 + \alpha_1} \pi \bar{K}$ .

(2) If  $\alpha_1 > \frac{1}{2}$ ,  $2k_0L \geq (G_1(iT) - G_1((i - j_1 + \frac{1}{2} + \pi - \alpha_1)T)) + (G_2(iT + \frac{T}{2}) - G_2((i - j_1 + \pi - \alpha_1)T)) + 2\pi TC = (j_1 - 1 + \frac{\alpha_1 - \frac{1}{2}}{\pi})\bar{g}_1T + (j_1 + \frac{\alpha_1 - \frac{1}{2}}{\pi})\bar{g}_2T + 2\pi TC = (2j_1 - 1 + \frac{2\alpha_1 - 1}{\pi})\bar{g}T + 2\pi TC$ .  
Thus  $k_0 \geq \frac{(j_1 + \frac{\alpha_1 - \frac{1}{2}}{\pi} + \frac{1}{2})\pi C}{(j_1 + \alpha_1)V} = \frac{j_1 + \frac{\alpha_1 - \frac{1}{2}}{\pi} + \frac{1}{2}}{j_1 + \alpha_1} \pi \bar{K}$ .

For sufficient conditions, we can get the same conclusion as the previous chapter similarly.

In summary, the first equation group (4.6a) is equivalent to  $k_0 \geq k_1$ . Similarly, we can prove that the second equation group (4.6b) is equivalent to  $k_0 \leq k_2$ .  $\square$

$k_1$  and  $k_2$  here are different from those in the previous chapter, because when there is no offset on the ring road, the most influential factors on  $k_1$  and  $k_2$  are the relationships between  $\alpha_1$ ,  $\alpha_2$  and  $\pi$ , while when there are offsets on the ring road, the most influential factors on  $k_1$  and  $k_2$  are the relationships between  $\alpha_1$ ,  $\alpha_2$  and  $\frac{\delta}{T}$ ,  $\pi$ .

When  $k_0 < k_1$ , then  $G_2((i - j_1 + \pi - \alpha_1)T) + k_0L < G_1(iT) + \pi TC$  and  $G_1((i - j_1 + \frac{1}{2} + \pi - \alpha_1)T) + k_0L < G_2(iT + \frac{T}{2}) + \pi TC$ , so we have

$$\begin{aligned} G_1(iT) + \bar{g}T &= G_2((i - j_1 + \pi - \alpha_1)T) + k_0L, \\ G_2(iT + \frac{T}{2}) + \bar{g}T &= G_1((i - j_1 + \frac{1}{2} + \pi - \alpha_1)T) + k_0L. \end{aligned}$$

When  $\alpha_1 \leq \frac{1}{2}$ ,  $\bar{g} = \frac{2k_0L}{(2j_1+1)T} = \frac{k_0}{k_1}\pi C$ .

When  $\alpha_1 > \frac{1}{2}$ , we assume that  $\bar{g}$  is also evenly distributed when  $\bar{g} < \pi C$ ,  $\bar{g} = \frac{2k_0L}{[2(j_1 + \frac{\alpha_1 - 0.5}{\pi}) + 1]T} = \frac{k_0}{k_1}\pi C$ .

So,  $\bar{g} \approx \frac{k_0}{k_1}\pi C$ . Similarly, when  $k_0 > k_2$ ,  $\bar{g} \approx \frac{K - k_0}{K - k_1}\pi C$ .

If  $k_1 \leq k_2$ , we have the same formula (3.10) for the MFD as the two-signal ring road without offset.

From the formula of MFD, we know that when  $k_1 \leq k_0 \leq k_2$ ,  $\bar{g}$  reaches the maximum

flow-rate  $\pi C$ , which is the capacity of the network, and  $\bar{g}$  can never exceed  $\pi C$  due to the influence of signals. However, when  $k_1 > k_2$ ,  $\bar{g}$  can never reach  $\pi C$ , and the actual capacity of the system will drop. This can happen only when  $T$  is very large compared to a specific link length  $L$ , which means  $j_1 + \alpha_1$  and  $j_2 + \alpha_2$  are very small. This is easy to understand, if  $T$  is very large, vehicles can go around the ring road only once during a cycle and spend the rest long time waiting at the signals because there is no overlap between the green time of the two signals, so  $\bar{g}$  is small.

**Lemma 4.2.** *The capacity drop of the network happens only when  $\frac{L}{VT} < \frac{1}{2}$  and  $\frac{L}{WT} < \frac{1}{2}$ .*

*Proof.*  $k_1 = \frac{j_1 + \max\{\frac{\alpha_1 - \frac{1}{2}}{\pi}, 0\} + \frac{1}{2}}{j_1 + \alpha_1} \pi \bar{K}$ , if  $\alpha_1 \geq \frac{1}{2}$ ,  $(j_1 + \frac{\alpha_1 - \frac{1}{2}}{\pi} + \frac{1}{2})\pi - (j_1 + \alpha_1) = (\pi - 1)(j_1 + \frac{1}{2}) < 0$ , which means  $k_1 < \bar{K}$ . If  $\alpha_1 < \frac{1}{2}$  and  $j_1 \geq 1$ ,  $\frac{(j_1 + \frac{1}{2})\pi}{j_1 + \alpha_1} \leq \frac{0.5(j_1 + \frac{1}{2})}{j_1} \leq \frac{0.5(1 + \frac{1}{2})}{1} = \frac{3}{4}$ , thus  $k_1 \leq \frac{3}{4}\bar{K} < \bar{K}$ . So when  $j_1 + \alpha_1 \geq \frac{1}{2}$ ,  $k_1 < \bar{K}$ . Similarly, when  $j_2 + \alpha_2 \geq \frac{1}{2}$ ,  $k_2 > \bar{K}$ .

If  $V \geq W$ , when  $j_1 = 0$ ,  $\alpha_1 \leq 0.5$  and  $j_2 + \alpha_2 > 0.5$ , we have  $k_1 = \frac{\frac{\pi}{2}CT}{L}$ ,  $k_2 = K - \frac{(\pi j_2 + \max\{\alpha_2 - \frac{1}{2} + \frac{\pi}{2}, \frac{\pi}{2}\})CT}{L}$ . If  $\alpha_2 \geq 0.5$ ,  $k_1 - k_2 \leq \frac{\frac{\pi}{2}CT}{L} + \frac{(\pi j_2 + \alpha_2 - \frac{1}{2} + \frac{\pi}{2})CT}{L} - K < \frac{(\alpha_1 + \frac{1}{2} - \frac{\pi}{2})CT}{L} + \frac{(j_2 + \alpha_2 - \frac{1}{2} + \frac{\pi}{2})CT}{L} - K = \frac{C}{V} + \frac{C}{W} - K = (\alpha_1 + \alpha_2)\frac{TC}{L} - K = 0$ , so  $k_1 < k_2$ . If  $\alpha_2 < 0.5$  and  $j_2 \geq 1$ ,  $k_1 - k_2 \leq \frac{\frac{\pi}{2}CT}{L} + \frac{(\pi j_2 + \frac{\pi}{2})CT}{L} - K = \frac{(\pi j_2 + \pi)C}{(j_2 + \alpha_2)W} - K < (K - \bar{K}) - K < 0$ , so  $k_1 < k_2$ .

If  $V < W$ , when  $j_2 = 0$ ,  $\alpha_2 \leq 0.5$  and  $j_1 + \alpha_1 > 0.5$ , similarly, we can get  $k_1 < k_2$ .

Consequently,  $\frac{L}{VT} = j_1 + \alpha_1 < \frac{1}{2}$  and  $\frac{L}{WT} = j_2 + \alpha_2 < \frac{1}{2}$  are necessary conditions for  $k_1 > k_2$ .  $\square$

**Corollary 4.3.** *When  $\frac{L}{VT} \geq \frac{1}{2}$  and  $\frac{L}{WT} \geq \frac{1}{2}$ ,  $k_1$  and  $k_2$  satisfy*

$$k_1 < \bar{K} < k_2. \quad (4.7)$$

Apart from the relationship in Corollary 4.3, we can also find the lower bound of  $k_1$  and the

upper bound of  $k_2$ .

**Lemma 4.4.** *When there is no capacity drop,  $k_1$  and  $k_2$  also satisfy*

$$\pi\bar{K} \leq k_1 \leq k_2 \leq K - \pi(K - \bar{K}), \quad (4.8)$$

and  $k_1 = \pi\bar{K}$  if and only if  $\alpha_1 = \frac{1}{2}$ ,  $k_2 = K - \pi(K - \bar{K})$  if and only if  $\alpha_2 = \frac{1}{2}$ .

*Proof.* If  $\alpha_1 < \frac{1}{2}$ ,  $j_1 + \frac{1}{2} > j_1 + \alpha_1$ , then  $k_1 > \pi\bar{K}$ , if  $\alpha_1 > \frac{1}{2}$ ,  $(j_1 + \frac{\alpha_1 - \frac{1}{2}}{\pi} + \frac{1}{2}) - (j_1 + \alpha_1) = (\alpha_1 - \frac{1}{2})(\frac{1}{\pi} - 1) > 0$ ,  $k_1 > \pi\bar{K}$ , if  $\alpha_1 = \frac{1}{2}$ ,  $k_1 = \frac{j_1 + \frac{1}{2}}{j_1 + \frac{1}{2}} \pi\bar{K} = \pi\bar{K}$ . So  $k_1 \geq \pi\bar{K}$ , and  $k_1 = \pi\bar{K}$  if and only if  $\alpha_1 = \frac{1}{2}$ . Similarly, we can prove that  $k_2 \leq K - \pi(K - \bar{K})$ , and  $k_2 = K - \pi(K - \bar{K})$  if and only if  $\alpha_2 = \frac{1}{2}$ .  $\square$

Consequently, when there is no capacity drop, if  $\frac{L}{V_T} \geq 0.5$ ,  $\frac{L}{W_T} \geq 0.5$ , the shape of MFD is the same as Figure 3.2, otherwise the shape of MFD is in Figure 4.2, because  $k_1 > \bar{K}$  or  $k_2 < \bar{K}$  will happen.

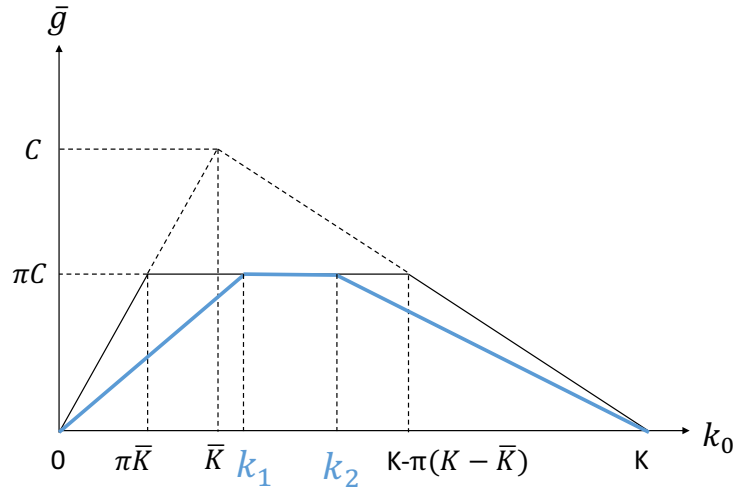


Figure 4.2: MFD of the two-signal ring road with offset (a)

### 4.2.2 Capacity of the system

Based on Lemma 4.2,  $k_1 > k_2$  is equivalent to  $\frac{\frac{1}{2}\pi CT}{L} > K - \frac{\frac{1}{2}\pi CT}{L}$ , thus  $L < \frac{\pi CT}{K}$ .

For the conditions when  $k_1 > k_2$ ,  $\bar{g}$  is maximized only when the equation group (4.9) is met, because in the LTM formulations (4.2a) and (4.3a), the first term  $G_a(t - \frac{L}{V}) + k_0L$  is positively correlated with  $k_0$ , while the second term  $G_a(t - \frac{L}{W}) + (K - k_0)L$  is negatively correlated with  $k_0$ .

$$\begin{aligned} G_1((i + \frac{1}{2} + \pi - \alpha_1)T) + k_0L &= G_1((i + \frac{1}{2} + \pi - \alpha_2)T) + (K - k_0)L, \\ G_2((i + \pi - \alpha_1)T) + k_0L &= G_2((i + \pi - \alpha_2)T) + (K - k_0)L. \end{aligned} \tag{4.9}$$

We can get  $k_0 = \frac{K}{2}$  from the equation group above because  $\alpha_1 \leq \frac{1}{2}$ ,  $\alpha_2 \leq \frac{1}{2}$ , and then

$$\begin{aligned} G_1((i + \pi)T) &= G_2((i - \frac{1}{2} + \pi)T) + \frac{KL}{2}, \\ G_2((i + \frac{1}{2} + \pi)T) &= G_1((i + \pi)T) + \frac{KL}{2}. \end{aligned}$$

So  $\bar{g} = \bar{g}_2 = \frac{KL}{T}$ , and for a specific  $T$ , the relationship between the system capacity  $c$  and the link length  $L$  is in Figure 4.3.

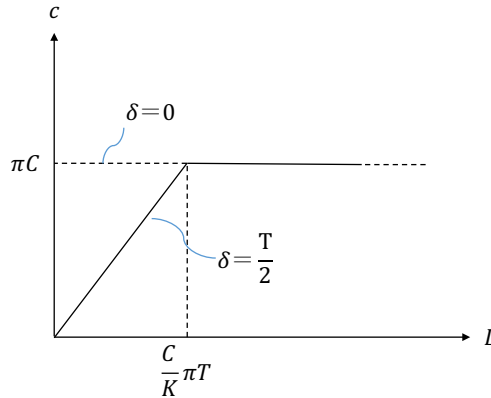


Figure 4.3: Capacity of the two-signal ring road with  $\pi \leq 0.5$

In addition, when the system capacity drops, the formula of the MFD is in (4.10), and the

shape of MFD is in Figure 4.4.

$$\bar{g}(k_0; T, \pi) \approx \begin{cases} \Phi_1(k_0; T, \pi), & 0 \leq k_0 < \frac{T}{2} \\ \Phi_2(k_0; T, \pi), & \frac{T}{2} \leq k_0 \leq K \end{cases} = \begin{cases} \frac{k_0}{k_1} \pi C, & 0 \leq k_0 < \frac{T}{2} \\ \frac{K-k_0}{K-k_1} \pi C, & \frac{T}{2} \leq k_0 \leq K \end{cases} \quad (4.10)$$

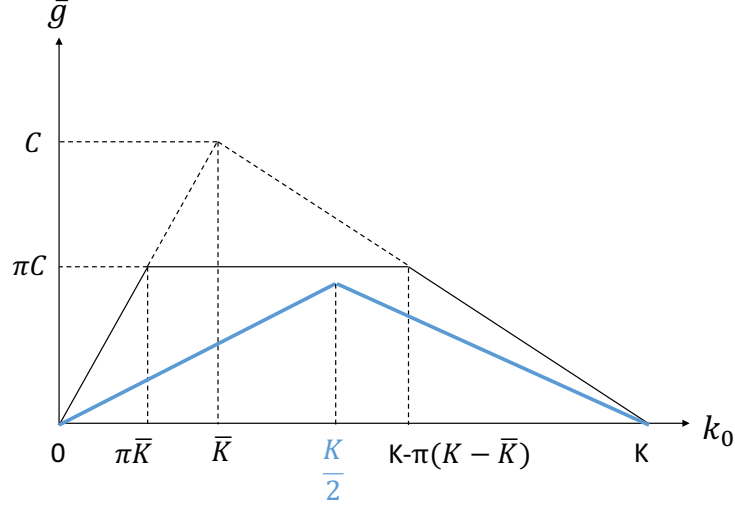


Figure 4.4: MFD of the two-signal ring road with offset (b)

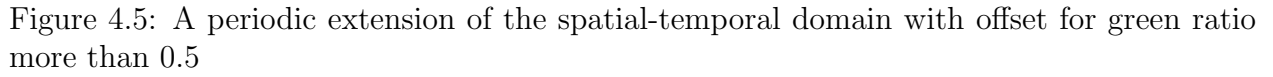
## 4.3 Conditions with a green ratio more than 0.5

### 4.3.1 Derivation of critical densities and MFD

When  $\pi > 0.5$ , we need to redefine the two critical densities as well:

$$k_1 = \frac{j_1 + L(\alpha_1) \frac{\alpha_1 - \frac{1}{2}}{\pi} + (1 - L(\alpha_1)) \min\{\frac{\alpha_1 + \frac{1}{2} - \pi}{\pi}, 0\} + \frac{1}{2} \pi \bar{K}}{j_1 + \alpha_1}, \quad (4.11a)$$

$$k_2 = K - \frac{j_2 + L(\alpha_2) \frac{\alpha_2 - \frac{1}{2}}{\pi} + (1 - L(\alpha_2)) \min\{\frac{\alpha_2 + \frac{1}{2} - \pi}{\pi}, 0\} + \frac{1}{2} \pi (K - \bar{K})}{j_2 + \alpha_2}, \quad (4.11b)$$

$$L(x) = \begin{cases} 1, & x > 0.5 \\ 0, & x \leq 0.5 \end{cases}$$


*Proof.* For the first equation group (4.6a), we have the following three scenarios:

(2) if  $\pi - 0.5 \leq \alpha_1 \leq 0.5$ ,  $2k_0L \geq (G_1(iT) - G_1((i - j_1 + \frac{1}{2} + \pi - \alpha_1)T)) + (G_2(iT + \frac{T}{2}) - G_2((i - j_1 + \pi - \alpha_1)T)) + 2\pi TC = (j_1 - 1)\bar{g}_1T + j_1\bar{g}_2T + 2\pi TC = (2j_1 - 1)\bar{g}T + 2\pi TC$ . Thus



$$k_0 \geq \frac{(j_1 + \frac{1}{2})\pi C}{(j_1 + \alpha_1)V} = \frac{j_1 + \frac{1}{2}}{j_1 + \alpha_1} \pi \overline{K}.$$

$$(3) \text{ if } \alpha_1 > 0.5, 2k_0L \geq (G_1(iT) - G_1((i - j_1 + \frac{1}{2} + \pi - \alpha_1)T)) + (G_2(iT + \frac{T}{2}) - G_2((i - j_1 + \pi - \alpha_1)T)) + 2\pi TC = (j_1 - 1 + \frac{\alpha_1 - 0.5}{\pi})\overline{g}_1T + (j_1 + \frac{\alpha_1 - 0.5}{\pi})\overline{g}_2T + 2\pi TC = (2j_1 - 1 + \frac{2\alpha_1 - 1}{\pi})\overline{g}T + 2\pi TC.$$

Thus  $k_0 \geq \frac{(j_1 + \frac{\alpha_1 - 0.5}{\pi} + \frac{1}{2})\pi C}{(j_1 + \alpha_1)V} = \frac{j_1 + \frac{\alpha_1 - 0.5}{\pi} + \frac{1}{2}}{j_1 + \alpha_1} \pi \overline{K}.$

For sufficient conditions, we can get the same conclusion as the previous chapter.

In summary, the first equation group (4.6a) is equivalent to  $k_0 \geq k_1$ . Similarly, we can prove that the second equation group (4.6b) is equivalent to  $k_0 \leq k_2$ .  $\square$

Compared to the previous section, we can find that  $k_1$  and  $k_2$  here are more complicated. When  $\pi \leq 0.5$ , there is no overlap between the green time of the two signals, while when there  $\pi > 0.5$ , there is overlap between the green time of the two signals, the overlapped time is  $\pi T - \delta$  during a cycle length. So  $k_1$  and  $k_2$  are also affected by the relationships between  $\alpha_1$ ,  $\alpha_2$  and  $\frac{\pi T - \delta}{T}$ .

$$\text{When } \pi - \frac{1}{2} \leq \alpha_1 \leq \frac{1}{2}, \overline{g} = \frac{2k_0L}{(2j_1 + 1)T} = \frac{k_0}{k_1} \pi C.$$

$$\text{When } \alpha_1 > \frac{1}{2}, \text{ we assume that } \overline{g} \text{ is also evenly distributed when } \overline{g} < \pi C, \overline{g} = \frac{2k_0L}{[2(j_1 + \frac{\alpha_1 - 0.5}{\pi}) + 1]T} = \frac{k_0}{k_1} \pi C.$$

$$\text{When } \alpha_1 < \pi - \frac{1}{2}, \text{ we also assume that } \overline{g} \text{ is also evenly distributed when } \overline{g} < \pi C, \overline{g} = \frac{2k_0L}{[2(j_1 + \frac{0.5 + \alpha_1 - \pi}{\pi}) + 1]T} = \frac{k_0}{k_1} \pi C.$$

$$\text{So, } \overline{g} \approx \frac{k_0}{k_1} \pi C. \text{ Similarly, when } k_0 > k_2, \overline{g} \approx \frac{K - k_0}{K - k_1} \pi C.$$

We also have the same formula as (3.10) for MFD when there is no capacity drop.

Lemma 4.2 is also established, when  $k_1 > k_2$ , we must have the conditions that  $\frac{L}{VT} < \frac{1}{2}$  and  $\frac{L}{WT} < \frac{1}{2}$ .

*Proof.*  $k_1 = \frac{j_1 + L(\alpha_1) \frac{\alpha_1 - \frac{1}{2}}{\pi} + (1 - L(\alpha_1)) \min\{\frac{\alpha_1 + \frac{1}{2} - \pi}{\pi}, 0\} + \frac{1}{2}}{j_1 + \alpha_1} \pi \bar{K}$ , if  $\alpha_1 \geq \frac{1}{2}$ ,  $(j_1 + \frac{\alpha_1 - \frac{1}{2}}{\pi} + \frac{1}{2})\pi - (j_1 + \alpha_1) = (\pi - 1)(j_1 + \frac{1}{2}) < 0$ , which means  $k_1 < \bar{K}$ . If  $\pi - 0.5 < \alpha_1 < \frac{1}{2}$  and  $j_1 \geq 1$ ,  $(j_1 + \frac{1}{2})\pi - (j_1 + \alpha_1) < (j_1 + \frac{1}{2})\pi - (j_1 + \pi - 0.5) = (\pi - 1)(j_1 - \frac{1}{2}) < 0$ , which means  $k_1 < \bar{K}$ . If  $\alpha_1 \leq \pi - 0.5$  and  $j_1 \geq 1$ ,  $(j_1 + \frac{\alpha_1 + \frac{1}{2} - \pi}{\pi} + \frac{1}{2})\pi - (j_1 + \alpha_1) = (\pi - 1)(j_1 - \frac{1}{2}) < 0$ , which means  $k_1 < \bar{K}$ . So that when  $j_1 + \alpha_1 \geq \frac{1}{2}$ ,  $k_1 < \bar{K}$ . Similarly, when  $j_2 + \alpha_2 \geq \frac{1}{2}$ ,  $k_2 > \bar{K}$ .

If  $V \geq W$ , when  $j_1 = 0$ ,  $\alpha_1 \leq 0.5$  and  $j_2 + \alpha_2 > 0.5$ ,  $k_1 = \frac{\min\{\alpha_1 + \frac{1}{2} - \frac{\pi}{2}, \frac{\pi}{2}\}CT}{L}$ ,  $k_2 = K - \frac{(\pi j_2 + L(\alpha_2)(\alpha_2 - \frac{1}{2} + \frac{\pi}{2}) + (1 - L(\alpha_2)) \min\{\alpha_2 + \frac{1}{2} - \frac{\pi}{2}, \frac{\pi}{2}\})CT}{L}$ , then  $k_1 - k_2 \leq \frac{(\alpha_1 + \frac{1}{2} - \frac{\pi}{2})CT}{L} + \frac{(\alpha_2 - \frac{1}{2} + \frac{\pi}{2})CT}{L} - K = (\alpha_1 + \alpha_2) \frac{TC}{L} - K = 0$ , so  $k_1 \leq k_2$ .

If  $V < W$ , when  $j_2 = 0$ ,  $\alpha_2 \leq 0.5$  and  $j_1 + \alpha_1 > 0.5$ , similarly, we can get  $k_1 \leq k_2$ .

Consequently,  $\frac{L}{VT} = j_1 + \alpha_1 < \frac{1}{2}$  and  $\frac{L}{WT} = j_2 + \alpha_2 < \frac{1}{2}$  are necessary conditions for  $k_1 > k_2$ .  $\square$

Corollary 4.3 and Lemma 4.4 are both established as well, which means  $k_1$  and  $k_2$  satisfy the same relationships, and we can also prove Lemma 4.4 when  $\pi > 0.5$ .

*Proof.* If  $\alpha_1 > \frac{1}{2}$ ,  $(j_1 + \frac{\alpha_1 - \frac{1}{2}}{\pi} + \frac{1}{2}) - (j_1 + \alpha_1) = (\alpha_1 - \frac{1}{2})(\frac{1}{\pi} - 1) > 0$ ,  $k_1 > \pi \bar{K}$ . If  $\pi - \frac{1}{2} < \alpha_1 < \frac{1}{2}$ ,  $(j_1 + \frac{1}{2}) > (j_1 + \alpha_1)$ ,  $k_1 \geq \pi \bar{K}$ . If  $\alpha_1 \leq \pi - \frac{1}{2}$ ,  $(j_1 + \frac{\alpha_1 + \frac{1}{2} - \pi}{\pi} + \frac{1}{2}) - (j_1 + \alpha_1) = (\alpha_1 + \frac{1}{2})(\frac{1}{\pi} - 1) > 0$ ,  $k_1 \geq \pi \bar{K}$ . If  $\alpha_1 = \frac{1}{2}$ ,  $k_1 = \frac{j_1 + \frac{1}{2}}{j_1 + \frac{1}{2}} \bar{K} = \bar{K}$ . So  $k_1 \geq \pi \bar{K}$ , and  $k_1 = \pi \bar{K}$  if and only if  $\alpha_1 = \frac{1}{2}$ . Similarly, we can prove that  $k_2 \leq K - (K - \bar{K})$ , and  $k_2 = K - \pi(K - \bar{K})$  if and only if  $\alpha_2 = \frac{1}{2}$ .  $\square$

So similar to the conditions with  $\pi \leq 0.5$ , when there is no capacity drop, the shapes of MFDs are in Figures 3.2 and 4.2. In addition, from the proof of Lemma 4.2, we can find that when  $\frac{L}{VT} \leq \pi - \frac{1}{2}$  and  $0.5 \leq \frac{L}{WT} \leq 1$ , or  $\frac{L}{WT} \leq \pi - \frac{1}{2}$  and  $0.5 \leq \frac{L}{VT} \leq 1$ ,  $k_1$  is always equal to  $k_2$ , so the shape of MFD is in Figure 4.6.

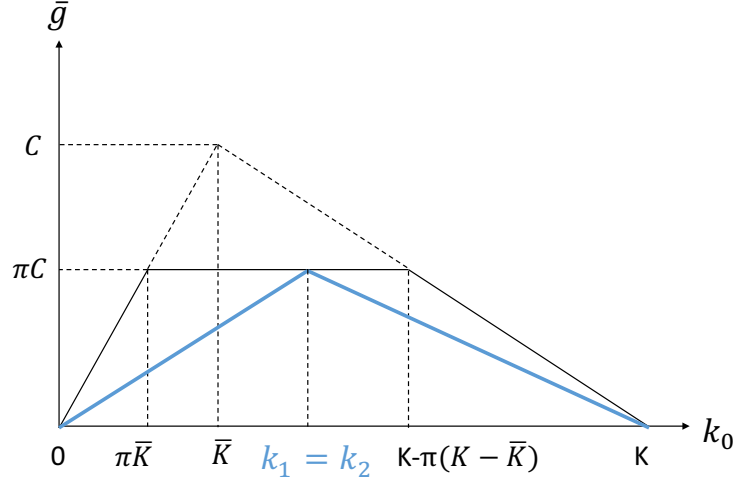


Figure 4.6: MFD of the two-signal ring road with offset (c)

### 4.3.2 Capacity of the system

We also need to find the critical point for  $k_1 \geq k_2$ , which means the system capacity begins to drop, and situations here are more complicated.

**Theorem 4.5.** *The conditions for the capacity drop are*

1. when  $\frac{V}{W} > \frac{1}{2\pi-1}$ ,  $L < \frac{CT}{2(K-\bar{K})}$ ,
2. when  $2\pi - 1 \leq \frac{V}{W} \leq \frac{1}{2\pi-1}$ ,  $L < \frac{\pi CT}{K}$ ,
3. when  $\frac{V}{W} < 2\pi - 1$ ,  $L < \frac{CT}{2\bar{K}}$ .

*Proof.* For  $V \geq W$ , when  $j_1 = j_2 = 0$ ,  $\alpha_1 \leq \alpha_2$ , if at the critical point,  $\alpha_1 \geq \pi - \frac{1}{2}$ , then  $k_1 > k_2$  is equivalent to  $\frac{\frac{1}{2}\pi CT}{L} + \frac{\frac{1}{2}\pi CT}{L} > K$ , thus  $L < \frac{\pi CT}{K} = \frac{C}{K}G$ , where  $G$  is the length of green time, and at the critical point,  $\alpha_1 = \frac{L}{VT} = \pi \frac{\bar{K}}{K} \geq \pi - \frac{1}{2}$ , so  $\frac{V}{W} \leq \frac{1}{2\pi-1}$ . If at the critical point,  $\alpha_1 < \pi - \frac{1}{2}$  while  $\alpha_2 \geq \pi - \frac{1}{2}$ , then  $\frac{(\frac{\alpha_1 + \frac{1}{2} - \pi}{\pi} + \frac{1}{2})\pi CT}{L} + \frac{\frac{1}{2}\pi CT}{L} > K$ , and  $\alpha_1 = \frac{L}{VT}$ , so  $L < \frac{CT}{2(K-\bar{K})}$ , and at the critical point,  $\alpha_1 = \frac{L}{VT} = \frac{\bar{K}}{2(K-\bar{K})} < \pi - \frac{1}{2}$ , so  $\frac{V}{W} > \frac{1}{2\pi-1}$ , and  $\alpha_2 = \frac{L}{WT} = \frac{1}{2} > \pi - \frac{1}{2}$  is automatically satisfied. If at the critical point,  $\alpha_1 < \pi - \frac{1}{2}$  and  $\alpha_2 < \pi - \frac{1}{2}$ , then  $\frac{(\frac{\alpha_1 + \frac{1}{2} - \pi}{\pi} + \frac{1}{2})\pi CT}{L} + \frac{(\frac{\alpha_2 + \frac{1}{2} - \pi}{\pi} + \frac{1}{2})\pi CT}{L} > K$ , because  $1 - \pi > 0$ , it is automatically

satisfied, which means no critical point exist under this condition.

When  $V < W$ , we can get the conditions for the capacity drop similarly.  $\square$

At the critical point,  $\bar{g}$  can still be equal to  $\pi C$  when (4.9) is met. So we can find the unique  $k_0$ , which is called  $k_c$  here, for  $\bar{g} = \pi C$ , and  $k_c = k_1 = k_2$ .

Then, the  $k_c$  for  $\bar{g} = \pi C$  on different conditions are

1. when  $\frac{V}{W} > \frac{1}{2\pi-1}$ ,  $k_c = \frac{K}{2} + \frac{\bar{K}}{2} - \frac{(\pi-\frac{1}{2})CT}{2L}$ ,
2. when  $2\pi - 1 \leq \frac{V}{W} \leq \frac{1}{2\pi-1}$ ,  $k_c = \frac{K}{2}$ ,
3. when  $\frac{V}{W} < 2\pi - 1$ ,  $k_c = \frac{K}{2} + \frac{(K-\bar{K})}{2} - \frac{(\pi-\frac{1}{2})CT}{2L}$ .

After finding the critical point, we can also find the relationship between  $L$  and the capacity of the system  $c$  for a specific  $T$ .

1. When the capacity drop happens with  $\alpha_1 < \pi - \frac{1}{2}$  and  $\alpha_2 < \pi - \frac{1}{2}$ , considering the capacity drop happens due to signal setting rather than density  $k_0$ , so at the beginning of the green time, we also have  $\bar{g}_1(t) = \pi C$  and  $\bar{g}_2(t) = \pi C$ . Then, based on (4.9), we have the relationships as follows:

$$\begin{aligned}
G_1((i + \pi)T) + (\pi - \frac{1}{2} - \alpha_1)CT + k_c L &= G_1((i + \pi)T) + (\pi - \frac{1}{2} - \alpha_2)CT + (K - k_c)L, \\
G_2((i - \frac{1}{2} + \pi)T) + (\pi - \frac{1}{2} - \alpha_1)CT + k_c L &= G_2((i - \frac{1}{2} + \pi)T) + (\pi - \frac{1}{2} - \alpha_2)CT \\
&+ (K - k_c)L.
\end{aligned}$$

We can get  $KL - 2k_c L = (\pi - \frac{1}{2} - \alpha_1)CT - (\pi - \frac{1}{2} - \alpha_2)CT = (\alpha_2 - \alpha_1)CT$ , so  $k_c =$

$\frac{K}{2} + (\alpha_1 - \alpha_2)\frac{CT}{2L} = \bar{K}$ , and then we have

$$\begin{aligned} G_1((i + \pi)T) &= G_2((i - \frac{1}{2} + \pi)T) + (\pi - \frac{1}{2} - \alpha_2)CT + (K - k_c)L, \\ G_2((i + \frac{1}{2} + \pi)T) &= G_1((i + \pi)T) + (\pi - \frac{1}{2} - \alpha_1)CT + k_cL. \end{aligned}$$

So  $\bar{g}T = \bar{g}_2T = 2(\pi - \frac{1}{2})CT - \frac{L}{VT}CT - \frac{L}{WT}CT + KL = 2(\pi - \frac{1}{2})CT$ . Thus  $\bar{g} = 2(\pi - \frac{1}{2})C$ .

2. When the capacity drop happens with  $\alpha_1 < \pi - \frac{1}{2}$  and  $\alpha_2 \geq \pi - \frac{1}{2}$ , we have

$$\begin{aligned} G_1((i + \pi)T) + (\pi - \frac{1}{2} - \alpha_1)CT + k_cL &= G_1((i + \pi)T) + (K - k_c)L, \\ G_2((i - \frac{1}{2} + \pi)T) + (\pi - \frac{1}{2} - \alpha_1)CT + k_cL &= G_2((i - \frac{1}{2} + \pi)T) + (K - k_c)L. \end{aligned}$$

We can get  $KL - 2k_cL = (\pi - \frac{1}{2} - \alpha_1)CT$ , so  $k_c = \frac{K}{2} + \frac{\bar{K}}{2} + (\frac{1}{2} - \pi)\frac{CT}{2L}$ , then we have

$$\begin{aligned} G_1((i + \pi)T) &= G_2((i - \frac{1}{2} + \pi)T) + (K - k_c)L, \\ G_2((i + \frac{1}{2} + \pi)T) &= G_1((i + \pi)T) + (\pi - \frac{1}{2} - \alpha_1)CT + k_cL. \end{aligned}$$

So  $\bar{g}T = (\pi - \frac{1}{2})CT - \frac{L}{VT}CT + KL = (\pi - \frac{1}{2})CT + (K - \bar{K})L$ . Thus  $\bar{g} = (\pi - \frac{1}{2})C + \frac{(K - \bar{K})}{T}L$ .

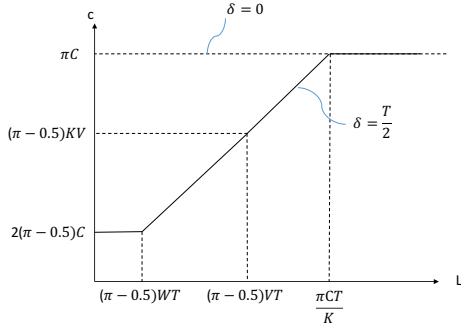
3. When the capacity drop happens with  $\alpha_2 < \pi - \frac{1}{2}$  and  $\alpha_1 \geq \pi - \frac{1}{2}$ , similar to Condition 2,  $k_c = \frac{K}{2} + \frac{K - \bar{K}}{2} + (\frac{1}{2} - \pi)\frac{CT}{2L}$ ,  $\bar{g} = (\pi - \frac{1}{2})C + \frac{\bar{K}L}{T}$ .

4. When the capacity drop happens with  $\alpha_1 \geq \pi - \frac{1}{2}$  and  $\alpha_2 \geq \pi - \frac{1}{2}$ , the result is the same as conditions with  $\pi \leq 0.5$ ,  $k_c = \frac{K}{2}$ ,  $\bar{g} = \frac{K}{T}L$ .

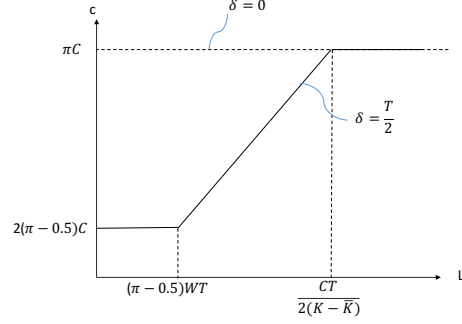
In summary, the relationships between  $L$  and  $c$  is in Figure 4.7:

- (1) The lower flat parts of four subfigures correspond to Condition 1,
- (2) The lower sloping part of subfigure (a) corresponds to Condition 2,
- (3) The lower sloping part of subfigure (c) corresponds to Condition 3,

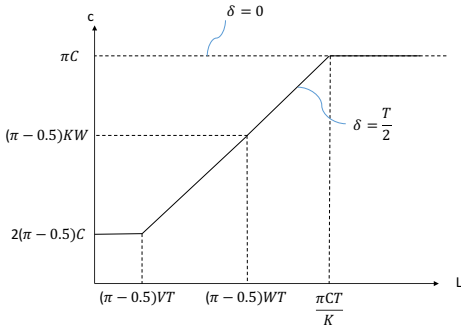
(4) The upper sloping part of subfigure (a), (c) and the sloping part of subfigure (b), (d) correspond to Condition 4.



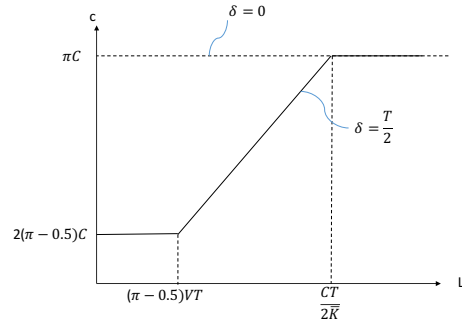
(a)  $V > W$  and  $\frac{V}{W} \leq \frac{1}{2\pi-1}$



(b)  $V > W$  and  $\frac{V}{W} > \frac{1}{2\pi-1}$



(c)  $V \leq W$  and  $\frac{V}{W} \geq 2\pi-1$



(d)  $V \leq W$  and  $\frac{V}{W} < 2\pi-1$

Figure 4.7: Capacity of the two-signal ring road with  $\pi > 0.5$

In [4], the capacity of the homogeneous two-signal ring road was derived by VT, with a special triangular fundamental diagram,  $V = \infty$ ,  $W = 1$ , and  $C = 1$ . The results are in accord with Figures 4.3 ( $\pi \leq 0.5$ ) and 4.7b ( $\pi > 0.5$ ).

When the system capacity drops, the formula of MFD is in (4.12), and the shape of MFD is

in Figure 4.8.

$$\bar{g}(k_0; T, \pi) \approx \begin{cases} \Phi_1(k_0; T, \pi), & 0 \leq k_0 < k_c \\ \Phi_2(k_0; T, \pi), & k_c \leq k_0 \leq K \end{cases} = \begin{cases} \frac{k_0}{k_1} \pi C, & 0 \leq k_0 < k_c \\ \frac{K-k_0}{K-k_1} \pi C, & k_c \leq k_0 \leq K \end{cases} \quad (4.12)$$

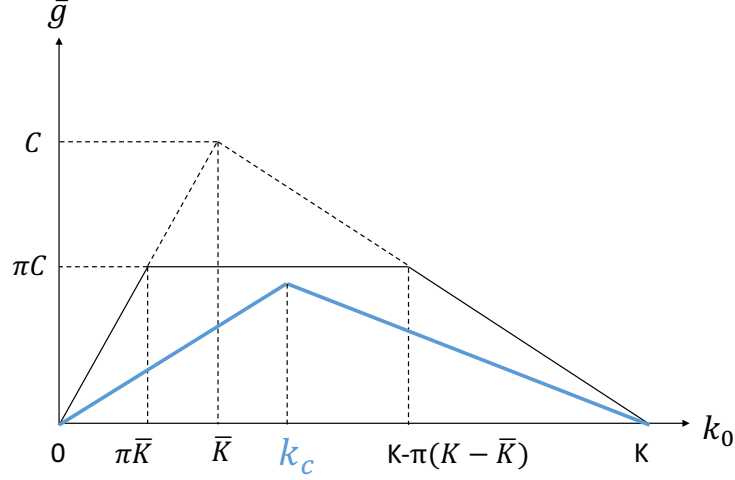


Figure 4.8: MFD of the two-signal ring road with offset (d)

There are four values for  $k_c$ ,

$$k_c \in \left\{ \bar{K}, \frac{K}{2}, \frac{K}{2} + \frac{\bar{K}}{2} + \left(\frac{1}{2} - \pi\right) \frac{CT}{2L}, \frac{K}{2} + \frac{K - \bar{K}}{2} + \left(\frac{1}{2} - \pi\right) \frac{CT}{2L} \right\},$$

and the value of  $k_c$  can be determined by the relationships of  $\alpha_1$ ,  $\alpha_2$  and  $\pi$ , based on the analysis of 4 conditions above.

# Chapter 5

## Optimal signal settings

In the previous chapter, we have understood the critical densities, approximate MFDs, and the variations of the capacity for two-signal ring road with offset. In this chapter, we can continue to study properties of the approximate MFD based on the result of Section 4, and then find the optimal cycle length for various situations.

### 5.1 Maximum flow-rate for various initial conditions

First, we should analyze the maximum flow-rate for a specific initial condition  $k_0$ . When  $T$  is no greater than critical point, which means there is no capacity drop, we can find the maximum flow-rate for different  $k_0$  in three regions:

1. When  $k_0 \in [0, \pi\bar{K})$ , since  $k_1 \geq \pi\bar{K}$ ,  $\bar{g} = \phi_1(k_0, T, \pi) = \frac{\pi C}{k_1} k_0$ ,  $\pi$  is fixed and decided by the ratio of flow-rate of all bounds in the intersection, when  $k_1$  is at minimum, which is  $\pi K$ ,  $\bar{g}$  is maximized. From Lemma 4.4, we know that  $k_1 = \pi\bar{K}$  only when  $\alpha_1 = 0.5$ , and then  $T = \frac{L}{V(j_1 + \frac{1}{2})}$ ,  $\bar{g}_{\max} = V k_0$ .



2. When  $k_0 \in [\pi\bar{K}, K - \pi(K - \bar{K})]$ , if  $j_1 + \alpha_1 \geq 0.5$ ,  $j_2 + \alpha_2 \geq 1$ ,  $k_1$  can reach  $\pi K$  and  $k_2$  can reach  $K - \pi(K - \bar{K})$ ,  $k_1$  and  $k_2$  are continuous on  $T$ , so for any  $k_0$ , we can find a  $T$  to make  $k_1 \leq k_0 \leq k_2$ , and  $\bar{g}_{\max} = \pi C$ .

3. When  $k_0 \in (K - \pi(K - \bar{K}), K]$ , since  $k_2 \leq K - \pi(K - \bar{K})$ ,  $\bar{g} = \phi_2(k_0, T, \pi) = \frac{\pi C}{K - k_2}(K - k_0)$ , when  $k_2$  is at maximum, which is  $K - \pi(K - \bar{K})$ ,  $\bar{g}$  is maximized. From Lemma 4.4, we know that  $k_2 = K - \pi(K - \bar{K})$  only when  $\alpha_2 = 0.5$ , and  $T = \frac{L}{V(j_2 + \frac{1}{2})}$ ,  $\bar{g}_{\max} = W(K - k_0)$ .

When  $T$  is greater than the critical point, there will be capacity drop, and the new capacity  $c$  of the system corresponds to  $k_c$ . There are only four values for  $k_c$ , so we can analyze the relationship between  $k_c$  and  $\pi\bar{K}$ ,  $K - \pi(K - \bar{K})$ .

1. When  $k_c = \bar{K}$ , apparently,  $\pi\bar{K} < k_c < K - \pi(K - \bar{K})$ .
2. When  $k_c = \frac{K}{2}$ , we have  $\pi \leq 0.5$ , or  $\pi > 0.5$  and  $2\pi - 1 \leq \frac{V}{W} \leq \frac{1}{2\pi - 1}$ . When  $\pi \leq 0.5$ ,  $\frac{K}{2} > \pi\bar{K}$ ,  $K - \pi(K - \bar{K}) - \frac{K}{2} > \pi\bar{K} > 0$ . When  $\pi > 0.5$  and  $2\pi - 1 \leq \frac{V}{W} \leq \frac{1}{2\pi - 1}$ ,  $\frac{K}{2} - \pi\bar{K} = \frac{K}{2} - \pi \frac{W}{V+W} K \geq \frac{W + (2\pi - 1)W - 2\pi W}{2(V+W)} K = 0$ ,  $K - \pi(K - \bar{K}) - \frac{K}{2} = \frac{K}{2} - \pi \frac{V}{V+W} K \geq \frac{V + (2\pi - 1)V - 2\pi V}{2(V+W)} K = 0$ .
3. When  $k_c = \frac{K}{2} + \frac{\bar{K}}{2} + (\frac{1}{2} - \pi) \frac{CT}{2L}$ , we have  $\pi > 0.5$ ,  $V \geq W$ ,  $L < \frac{CT}{2(K - \bar{K})}$  and  $\frac{L}{WT} \geq \pi - \frac{1}{2}$ .  $k_c - \pi\bar{K} \geq \frac{K}{2} + \frac{\bar{K}}{2} - \frac{CT}{2WT} - \pi\bar{K} = \bar{K} - \pi\bar{K} > 0$ .  $K - \pi(K - \bar{K}) - k_c \geq K - \pi(K - \bar{K}) - \frac{K}{2} - \frac{\bar{K}}{2} + (\pi - \frac{1}{2})2(K - \bar{K}) = (\pi - \frac{1}{2})(K - \bar{K}) > 0$ .
4. When  $k_c = \frac{K}{2} + \frac{K - \bar{K}}{2} + (\frac{1}{2} - \pi) \frac{CT}{2L}$ , similar to Condition 3, we can prove that  $k_c - \pi\bar{K} > 0$  and  $K - \pi(K - \bar{K}) - k_c > 0$ .

In summary,  $\pi\bar{K} < k_c < K - \pi(K - \bar{K})$ , which means in Figures 4.4 and 4.8, the thick blue lines are always below the thin black solid lines. So the maximum flow-rate for any  $k_0$  can only happen when there is no capacity drop.

## 5.2 Optimal cycle lengths

After analyzing the maximum flow-rate of the system under various conditions, we can try to find a optimal cycle length  $T$  for different  $k_0$ . In reality, the green time consists of the effective green time and the lost time, so we introduce the lost time  $l$ , which can be seen as the same for all phases in the intersection. For an intersection without turning movements, there are two phases and the effective green time  $\pi T$  will be  $(T - 2l)\pi_0$ , where,  $\pi_0$  is the initial green ratio, which is determined by the demand of two phases, and  $\pi$  is the effective green ratio:

$$\pi = (1 - \frac{2l}{T})\pi_0 \quad (5.1)$$

If  $T$  is too small, the effective green ratio  $\pi$  will be small and most of the green time is wasted. In contrast, if  $T$  is too large, the capacity of the ring road will drop because most of the green time is wasted, as discussed in Chapter 4. So we should find a cycle length that can maximize the system's flow-rate  $\bar{g}$  by considering the effect of the lost time  $l$ :

1. When  $k_0 \in [0, \pi\bar{K})$ ,  $\bar{g}_{max} \approx Vk_0$ , and is not related to the green ratio, so that the optimal cycle lengths are

$$T^* = \frac{L}{V(j_1 + \frac{1}{2})} \quad (5.2)$$

where  $j_1 = 0, 1, 2, \dots$ , and  $Vk_0 \leq (1 - \frac{2l}{T^*})\pi_0 C$ .

2. When  $k_0 \in [\pi\bar{K}, K - \pi(K - \bar{K})]$ , if  $j_1 + \alpha_1 \geq \frac{1}{2}$  and  $j_2 + \alpha_2 \geq \frac{1}{2}$ , for any  $k_0$ , there will be a  $T$  to make  $\bar{g} = \pi C = (1 - \frac{2l}{T})\pi_0 C$ . However, to mitigate the influence of lost time  $l$ , we hope to make  $T$  as large as possible before the capacity drop happens, which means we need  $j_1 + \alpha_1 \leq \frac{1}{2}$ , or  $j_2 + \alpha_2 \leq \frac{1}{2}$ .

(1)  $\pi_0 \leq 0.5$ , or  $\pi_0 > 0.5$ , and  $2\pi_0 - 1 \leq \frac{V}{W} \leq \frac{1}{2\pi_0 - 1}$ .

Under these conditions,  $k_c = \frac{K}{2}$ , so  $k_1$  and  $k_2$  will converge to  $\frac{K}{2}$  before the capacity begins to drop.

When  $k_0 < \frac{K}{2}$ ,  $\bar{g}_{max}$  is determined by  $\phi_1$  and  $\pi C$ , so that

$$\bar{g}^* = \max_{T \in [\frac{2L}{V}, \frac{KL}{\pi C}]} \min\{\frac{\pi C}{0.5\pi C} k_0, (1 - \frac{2l}{T})\pi_0 C\} = \max_{T \in [\frac{2L}{V}, \frac{KL}{\pi C}]} \min\{\frac{L}{0.5T} k_0, (1 - \frac{2l}{T})\pi_0 C\},$$

so the optimal cycle length is

$$T^* = \frac{2k_0 L}{\pi_0 C} + 2l.$$

When  $k_0 \geq \frac{K}{2}$ ,  $\bar{g}_{max}$  is determined by  $\phi_2$  and  $\pi C$ , so that

$$\bar{g}^* = \max_{T \in [\frac{2L}{W}, \frac{KL}{\pi C}]} \min\{\frac{\pi C}{0.5\pi C} (K - k_0), (1 - \frac{2l}{T})\pi_0 C\} = \max_{T \in [\frac{2L}{W}, \frac{KL}{\pi C}]} \min\{\frac{L}{0.5T} (K - k_0), (1 - \frac{2l}{T})\pi_0 C\},$$

so the optimal cycle length is

$$T^* = \frac{2(K - k_0)L}{\pi_0 C} + 2l.$$

(2)  $\pi_0 > 0.5$ , and  $\frac{V}{W} \geq \frac{1}{2\pi_0 - 1}$ .

We have  $k_c = \frac{K}{2} + \frac{\bar{K}}{2} - \frac{(\pi - \frac{1}{2})CT}{2L}$ .

When  $k_0 \leq \frac{\pi_0 \bar{K}}{2\pi_0 - 1}$ , the optimal cycle length is the same as before,

$$T^* = \frac{2k_0 L}{\pi_0 C} + 2l.$$

When  $\frac{\pi_0 \bar{K}}{2\pi_0 - 1} < k_0 \leq \frac{K}{2} + \frac{\bar{K}}{2} - \frac{(\pi_0 - \frac{1}{2})CT}{2L}$ ,  $\bar{g}_{max}$  is also determined by  $\phi_1$  and  $\pi C$ ,

$$\begin{aligned}\bar{g}^* &= \max_{T \in [\frac{2L}{V(2\pi-1)}, \frac{2(K-\bar{K})L}{C}]} \min\left\{\frac{\pi C}{\frac{(\frac{L}{VT} + \frac{1}{2} - \frac{\pi}{2})\pi C}{\frac{L}{T}}} k_0, (1 - \frac{2l}{T^*})\pi_0 C\right\} \\ &= \max_{T \in [\frac{2L}{V(2\pi-1)}, \frac{2(K-\bar{K})L}{C}]} \min\left\{\frac{\pi L}{(\frac{L}{VT} + \frac{1}{2} - \frac{\pi}{2})T} k_0, (1 - \frac{2l}{T})\pi_0 C\right\},\end{aligned}$$

and  $\pi = (1 - \frac{2l}{T})\pi_0$ , so the optimal cycle length is

$$T^* = \frac{2[(\frac{k_0}{C} - \frac{1}{V})L - l\pi_0]}{1 - \pi_0}.$$

When  $k_0 > \frac{K}{2} + \frac{\bar{K}}{2} - \frac{(\pi_0 - \frac{1}{2})CT}{2L}$ , the optimal cycle length is the same as before,

$$T^* = \frac{2(K - k_0)L}{\pi_0 C} + 2l.$$

(3)  $\pi_0 > 0.5$ , and  $\frac{V}{W} \leq 2\pi_0 - 1$ .

We have  $k_c = \frac{K}{2} + \frac{(K-\bar{K})}{2} - \frac{(\pi - \frac{1}{2})CT}{2L}$ .

When  $k_0 \leq \frac{K}{2} + \frac{(K-\bar{K})}{2} - \frac{(\pi_0 - \frac{1}{2})CT}{2L}$ , the optimal cycle length is the same as before,

$$T^* = \frac{2k_0 L}{\pi_0 C} + 2l.$$

When  $\frac{K}{2} + \frac{(K-\bar{K})}{2} - \frac{(\pi_0 - \frac{1}{2})CT}{2L} < k_0 \leq K - \frac{\pi_0(K-\bar{K})}{2\pi_0 - 1}$ ,  $\bar{g}_{max}$  is also determined by  $\phi_2$  and  $\pi C$ ,

$$\begin{aligned}\bar{g}^* &= \max_{T \in [\frac{2L}{W(2\pi-1)}, \frac{2\bar{K}L}{C}]} \min\left\{\frac{\pi C}{\frac{(\frac{L}{WT} + \frac{1}{2} - \frac{\pi}{2})\pi C}{\frac{L}{T}}} (K - k_0), (1 - \frac{2l}{T^*})\pi_0 C\right\} \\ &= \max_{T \in [\frac{2L}{W(2\pi-1)}, \frac{2\bar{K}L}{C}]} \min\left\{\frac{\pi L}{(\frac{L}{WT} + \frac{1}{2} - \frac{\pi}{2})T} (K - k_0), (1 - \frac{2l}{T})\pi_0 C\right\},\end{aligned}$$

so the optimal cycle length is

$$T^* = \frac{2[(\frac{K-k_0}{C} - \frac{1}{W})L - l\pi_0]}{1 - \pi_0}.$$

When  $k_0 \geq K - \frac{\pi(K-\bar{K})}{2\pi_0-1}$ , the optimal cycle length is the same as before,

$$T^* = \frac{2(K - k_0)L}{\pi_0 C} + 2l.$$

In summary, for  $k_0 \in [\pi\bar{K}, K - \pi(K - \bar{K})]$ ,

(1) when

(a)  $\pi_0 \leq 0.5$ , or  $\pi_0 > 0.5$ ,  $2\pi_0 - 1 \leq \frac{V}{W} \leq \frac{1}{2\pi_0-1}$ , and  $k_0 < \frac{K}{2}$ ,

(b)  $\pi_0 > 0.5$ ,  $\frac{V}{W} \geq \frac{1}{2\pi_0-1}$ , and  $k_0 \leq \frac{\pi_0 \bar{K}}{2\pi_0-1}$ ,

(c)  $\pi_0 > 0.5$ ,  $\frac{V}{W} \leq 2\pi_0 - 1$ , and  $k_0 \leq \frac{K}{2} + \frac{(K-\bar{K})}{2} - \frac{(\pi_0-\frac{1}{2})CT}{2L}$ ,

the optimal cycle length is

$$T^* = \frac{2k_0 L}{\pi_0 C} + 2l. \tag{5.3}$$

(2) When

(a)  $\pi_0 \leq 0.5$ , or  $\pi_0 > 0.5$ ,  $2\pi_0 - 1 \leq \frac{V}{W} \leq \frac{1}{2\pi_0-1}$ , and  $k_0 \geq \frac{K}{2}$ ,

(b)  $\pi_0 > 0.5$ ,  $\frac{V}{W} \geq \frac{1}{2\pi_0-1}$ , and  $k_0 > \frac{K}{2} + \frac{\bar{K}}{2} - \frac{(\pi_0-\frac{1}{2})CT}{2L}$ ,

(c)  $\pi_0 > 0.5$ ,  $\frac{V}{W} \leq 2\pi_0 - 1$ , and  $k_0 \geq K - \frac{\pi(K-\bar{K})}{2\pi_0-1}$ ,

the optimal cycle length is

$$T^* = \frac{2(K - k_0)L}{\pi_0 C} + 2l. \tag{5.4}$$

(3) When  $\pi_0 > 0.5$ ,  $\frac{V}{W} \geq \frac{1}{2\pi_0-1}$ , and  $\frac{\pi_0 \bar{K}}{2\pi_0-1} < k_0 \leq \frac{K}{2} + \frac{\bar{K}}{2} - \frac{(\pi_0 - \frac{1}{2})CT}{2L}$ ,

the optimal cycle length is

$$T^* = \frac{2[(\frac{k_0}{C} - \frac{1}{V})L - l\pi_0]}{1 - \pi_0}. \quad (5.5)$$

(4) When  $\pi_0 > 0.5$ ,  $\frac{V}{W} \leq 2\pi_0 - 1$ , and  $\frac{K}{2} + \frac{(K-\bar{K})}{2} - \frac{(\pi_0 - \frac{1}{2})CT}{2L} < k_0 \leq K - \frac{\pi_0(K-\bar{K})}{2\pi_0-1}$ ,

the optimal cycle length is

$$T^* = \frac{2[(\frac{K-k_0}{C} - \frac{1}{W})L - l\pi_0]}{1 - \pi_0}. \quad (5.6)$$

3. When  $k_0 \in (K - \pi(K - \bar{K}), K]$ ,  $\bar{g}_{max} \approx W(K - k_0)$ , and is not related to the green ratio either, so that the optimal cycle lengths are

$$T^* = \frac{L}{V(j_2 + \frac{1}{2})} \quad (5.7)$$

where  $j_2 = 0, 1, 2, \dots$ , and  $W(K - k_0) \leq (1 - \frac{2l}{T^*})\pi_0 C$ .

# Chapter 6

## Numerical Simulation

In the previous chapters, we have analyzed the two-signal ring road theoretically, in this chapter, we will develop discrete LIM formulas and apply them to numerical simulations to test the theoretical results.

Discretize the demand and supply functions in (2.4) into every time-step  $\Delta t$ , then the discrete demand and supply functions for Link  $a$  are

$$d_a(t)\Delta t = \begin{cases} \min \{(t + \Delta t)k_0V - G_a(t), C\Delta t\}, & t + \Delta t \leq \frac{L}{V} \\ \min \{G_{a-1}(t + \Delta t - \frac{L}{V}) - G_a(t) + k_0L, C\Delta t\}, & t + \Delta t > \frac{L}{V} \end{cases} \quad (6.1a)$$

$$s_a(t)\Delta t = \begin{cases} \min \{(t + \Delta t)(K - k_0)W - G_{a-1}(t), C\Delta t\}, & t + \Delta t \leq \frac{L}{W} \\ \min \{G_a(t + \Delta t - \frac{L}{W}) + (K - k_0)L - G_{a-1}(t), C\Delta t\}, & t + \Delta t > \frac{L}{W} \end{cases} \quad (6.1b)$$

The discrete boundary flow-rate at Signal  $a$  is

$$g_a(t)\Delta t = \beta_a(t) \min \{d_a(t)\Delta t, s_{a-1}(t)\Delta t\}. \quad (6.2)$$

The logic of simulations (with offset) is represented by flowcharts, in Figures 6.1 and 6.2.

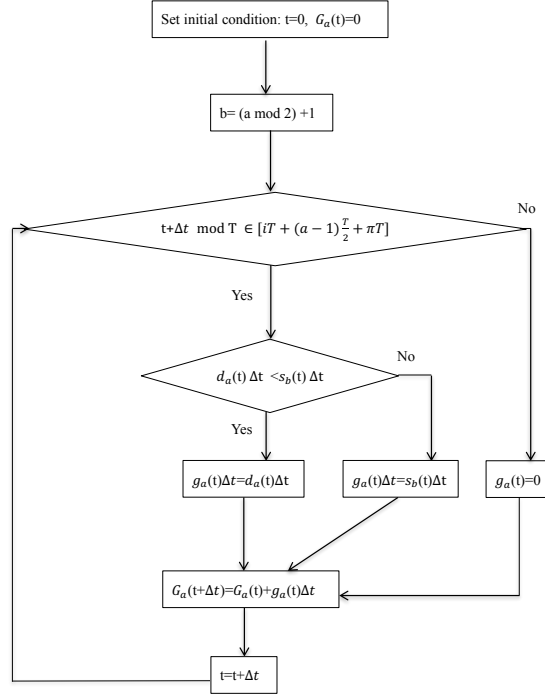


Figure 6.1: Flow chart of  $G_a$  and  $g_a$

## 6.1 Convergency

In [10], it was mathematically proven that in the signalized ring road, there exists asymptotic convergency patterns. In this section, we can also test whether the conclusion holds in the two-signal ring road by numerical simulations.

We check the convergency of the average flow-rate  $\bar{g}$  of the total simulation time for different total simulation time  $\tau$  and different time step sizes  $\Delta t$ . In this section, we use a unitless triangular fundamental diagram with  $V = 1, W = 0.25, K = 1, C = 0.2$ , and the link length  $L = 100$ .

First, we set  $\Delta t = 1$ , and  $\tau$  equals  $10^5, 10^6, 10^7, 10^8, 10^9$ , respectively. The error  $E$  is the difference between the average flow-rates of the first 4  $\tau$  and  $\tau = 10^9$  respectively. We have 5 conditions with different cycle lengths  $T$  or green ratios  $\pi$ . The results are in Figure 6.3,



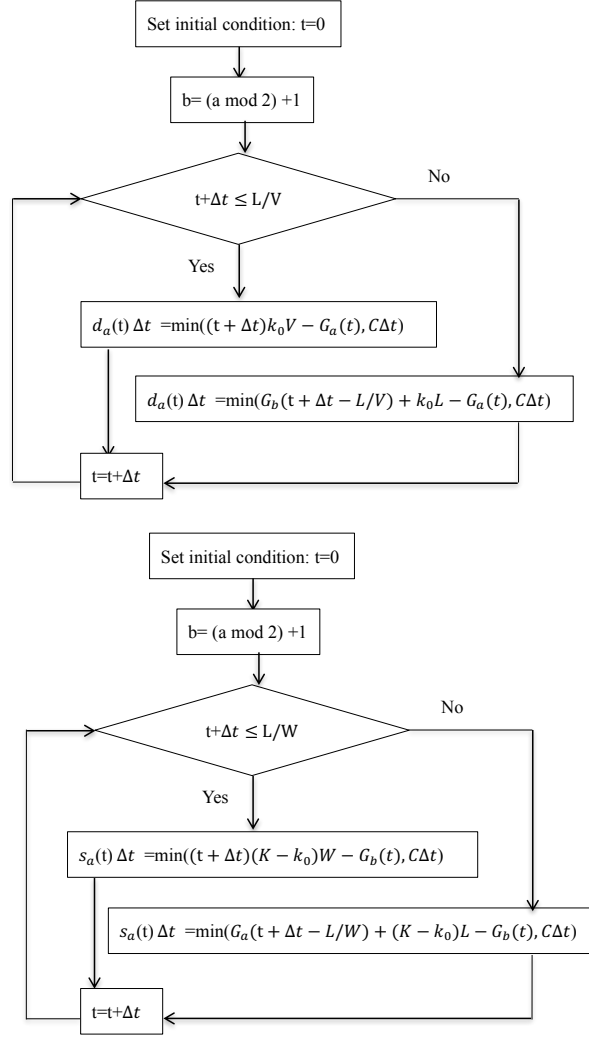
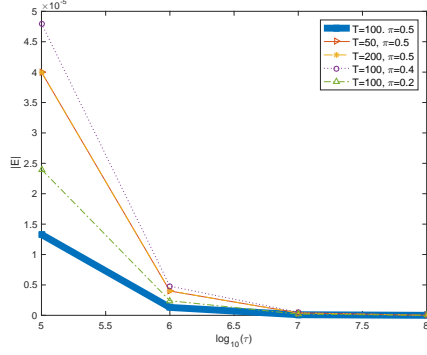


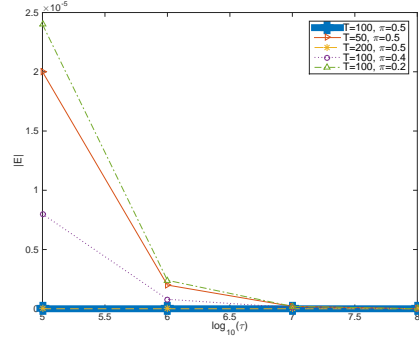
Figure 6.2: Flow charts of  $d_a$  and  $s_a$

we can see that the errors monotonously decrease as  $\tau$  increases. When  $\tau = 10^8$ , the errors are 0 on various conditions. So we can believe that as  $\tau$  becomes larger, the convergency pattern is similar:  $\bar{g}$  will be constant when  $\tau$  is large enough.

Secondly, we set  $\tau = 10^5$ , and  $\Delta t$  equals 10, 1, 0.1, 0.01, 0.001, 0.0001, respectively. The error  $E$  is the difference between the average flow-rates of the first 5  $\Delta t$  and  $\Delta t = 0.0001$  respectively. We also have the same 5 conditions as before. The results are in Figure 6.4, we can find that as  $\Delta t$  becomes smaller, the  $E$  will all be 0 at last, and  $\bar{g}$  will be constant



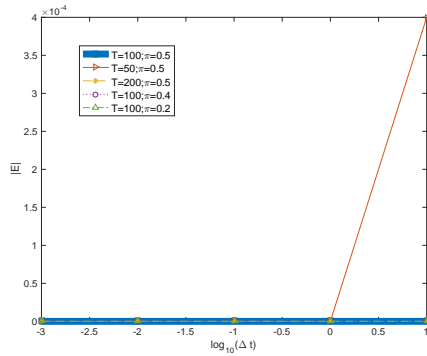
(a) Without offset



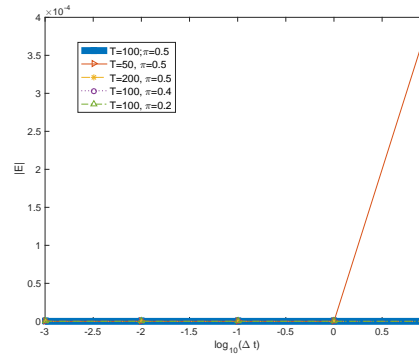
(b) With offset

Figure 6.3: Convergence of the LTM with respect to total simulation time

when  $\Delta t$  is small enough.



(a) Without offset



(b) With offset

Figure 6.4: Convergence of the LTM with respect to time-step size

Consequently, based on the the results of tests on  $\tau$  and  $\Delta t$ , the convergency patterns on the two-signal ring road exist.

## 6.2 Minimum period

Asymptotic periodic traffic patterns also exist on the signalized ring road ([10]), although we assume that the minimum period of the signalized ring road equals the cycle length, actually,

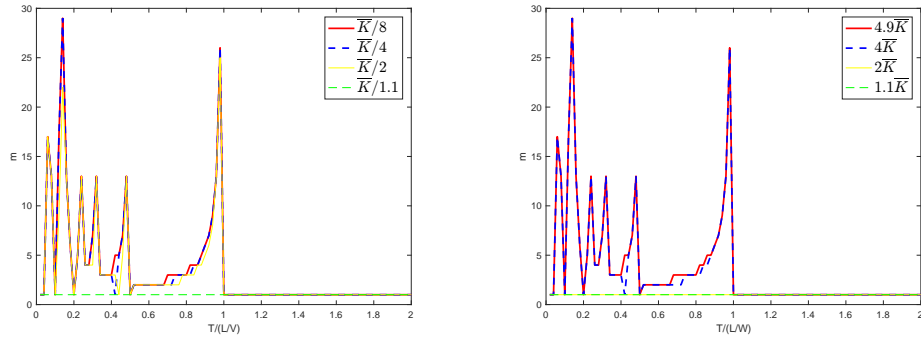
when  $\bar{g} < \pi C$  and  $T$  is small, the exact minimum period may be  $mT$ , an integer multiple of the cycle length, so we can find the real minimum period for various conditions by numerical simulation methods. Set  $\tau = 10^6$ ,  $\Delta t = 1$ , the  $m$  is the smallest integer that satisfies:

$$\max_{t \in (\tau - mT, \tau]} |g_1(t - mT) - g_1(t)| < 10^{-5}, \quad (6.3a)$$

$$\max_{t \in (\tau - mT, \tau]} |g_2(t - mT) - g_2(t)| < 10^{-5}. \quad (6.3b)$$

The fundamental diagram used is the same as the previous section.

First, we set  $\pi = 0.5$  and find the minimum period of the two-signal ring road without offset, and from the results of various  $k_0$  (Figure 6.5), we can find that: (a) when  $k_0 < \bar{K}$  and  $T/(L/V) \geq 1$ , or  $k_0 > \bar{K}$  and  $T/(L/W) \geq 1$ , the minimum period always equals the cycle length, (b) when  $k_0 \approx \bar{K}$  and  $T$  is not large, the minimum period always equals the cycle length, (c) except the conditions in (a) and (b),  $m$  may be greater than 1.



(a) Without offset and  $k_0 \in (0, \bar{K})$       (b) Without offset and  $k_0 \in (\bar{K}, K)$

Figure 6.5: The periods with respect to multiple times of the cycle length (a)

Secondly, we set  $k_0$  equal to  $\bar{K}/8$  and  $4.9\bar{K}$ , respectively, and find the minimum period of the two-signal ring road without offset for various  $\pi$ . From the results (Figure 6.6), we can find that when  $\pi$  is greater,  $T$  should be larger so that  $m$  can always equal 1, and the maximum of  $m$  can be larger.

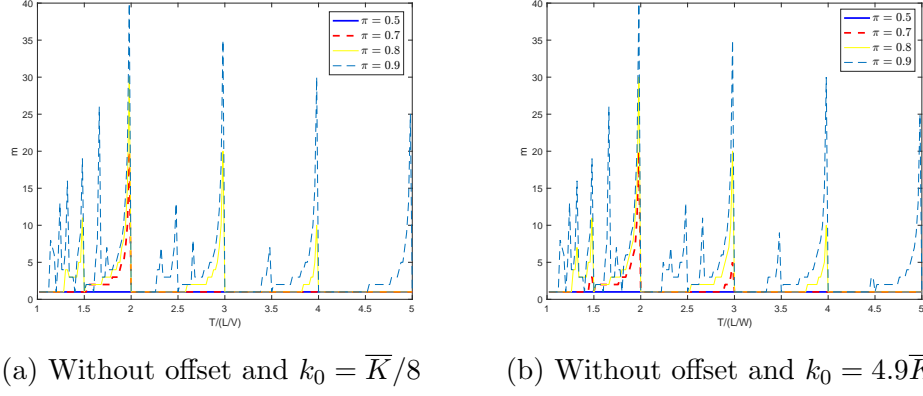


Figure 6.6: The periods with respect to multiple times of the cycle length (b)

Thirdly, we set  $\pi = 0.5$  and find the minimum period of the two-signal ring road with offset, the results of various  $k_0$  are in Figure 6.7. We can find that when  $T/(L/V) \geq 2$  for low initial densities and  $T/(L/W) \geq 2$  for high initial densities, the minimum period always equal the cycle length. So compared to the two-signal ring road without offset,  $T$  should be larger so that  $m$  can always equal 1. In addition, for conditions when  $m$  can be greater than 1, the maximum of  $m$  is much larger.

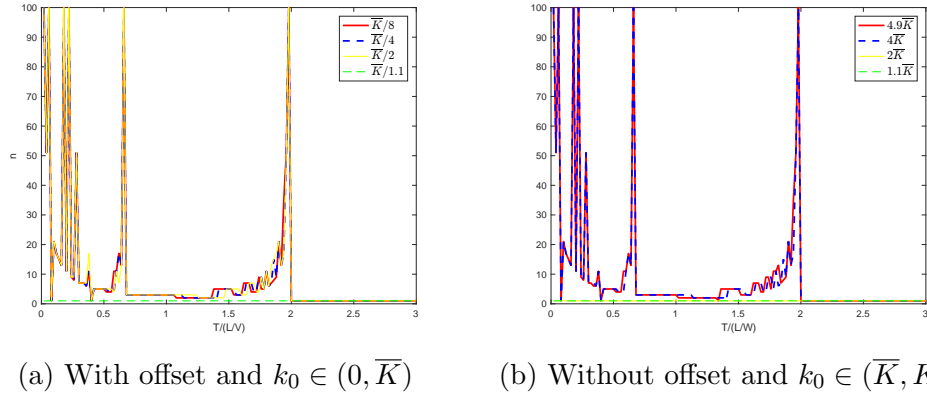


Figure 6.7: The periods with respect to multiple times of the cycle length (c)

### 6.3 MFDs from simulation

After testing the convergency patterns and finding the periodical pattern of the system, we can get MFDs by calculating  $\bar{g}$  for the one-signal ring road and  $\bar{g}_1$  for the two-signal ring road when  $\tau$  is large,  $\bar{g}$  and  $\bar{g}_1$  are defined as follows:

$$\bar{g}(k_0; T, \pi) = \frac{\int_{\tau-mT}^{\tau} g(t) dt}{mT}, \quad (6.4a)$$

$$\bar{g}_1(k_0; T, \pi, \delta) = \frac{\int_{\tau-mT}^{\tau} g_1(t) dt}{mT}, \quad (6.4b)$$

where  $g(t)$  is the boundary flow-rate of the one-signal ring road.

In this section, we use a triangular fundamental diagram, with  $V = 20m/s$ ,  $W = 5m/s$ ,  $K = 1/7veh/s$ . We also consider the effects of the lost time  $l$  for each phase, and empirically  $l = 3s$ . For the one-signal ring road and the two-signal ring road without offset, the link length  $L = 1200m$ , while for the two-signal ring road with offset,  $L = 600m$ . The latter's link length is smaller so as to show the capacity drop phenomenon better when  $T$  is comparatively large.

For different cycle lengths and green ratios, MFDs of one-signal ring road and two-signal ring road without offset, and MFDs of two-signal ring road with offset are in Figures 6.8 and 6.9 respectively. First, we can find that for the same cycle length and green ratio, the two MFDs of one-signal ring road and two-signal ring road without offset are exactly overlapped, so that from both theoretical and numerical results, we can conclude that the one-signal ring road and the two-signal ring road without offset are essentially the same. Secondly, as mentioned in [11], we can find that when  $k_0 < k_1$ , and  $k_0 > k_2$ , the functions of  $\bar{g}(k_0; T, \pi, \delta)$  are not linear, so the trapezoidal or triangular MFDs are just a kind of approximation, but is still good enough since the difference between approximation and accurate results are not big. Thirdly, from MFDs of two-signal ring road with offset, we can find that when  $T$  is

large enough, the capacity drop will happen, and the dropped capacity happens at  $k_0 = \frac{1}{2}K$  ( $\pi \leq 0.5$ ).

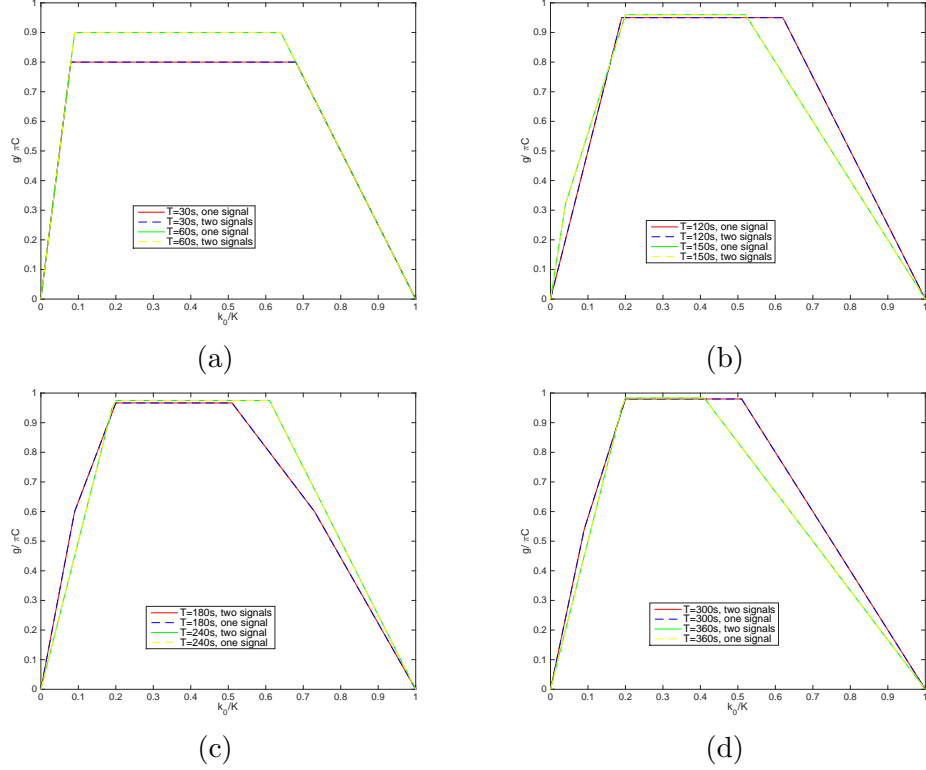


Figure 6.8: Simulated MFD of the one-signal ring road and the two-signal without offset

## 6.4 Relationship between capacity and link length

In this section, we will study the capacity drop phenomena numerically and verify the relationships between the capacity  $c$  and link length  $L$  from the theoretical derivation in Chapter 4. The fundamental diagram used is the same as the first section and the cycle length  $T = 400$ . We search  $\bar{g}$  from  $k_0 = 0$  to  $k_0 = K$  to get the the maximum average flow-rate  $\bar{g}$  as the capacity  $c$  for different link lengths. For conditions when  $\pi \leq 0.5$ , search  $\bar{g}$  by every  $0.01K$  is enough to find accurate capacity for different  $L$ , because  $k_c = \frac{1}{2}K$ . However, when  $\pi > 0.5$ ,  $k_c$  may not be an integer multiple of  $0.01K$ , so only searching  $\bar{g}$  by every  $0.01K$  is

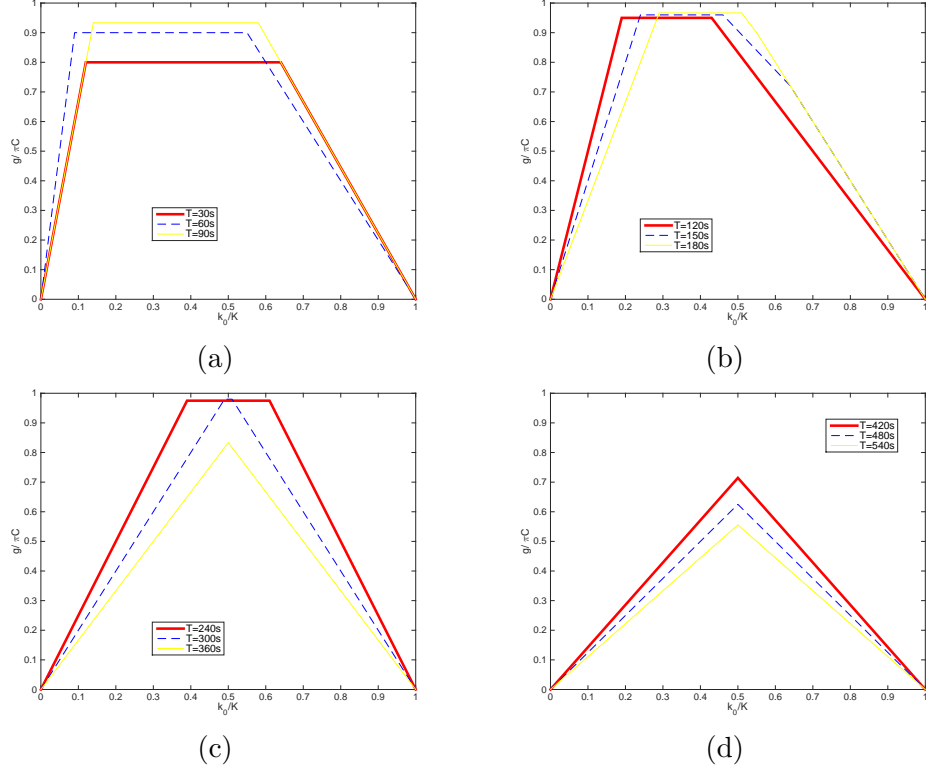


Figure 6.9: Simulated MFD of the two-signal ring road with offset

not enough to get the accurate  $c$ . Considering the triangular MFD is unimodal, first search  $\bar{g}$  by every  $0.01K$ , and find the interval of length  $0.02K$ , on which  $k_c$  falls, by selecting the biggest three  $\bar{g}$ , then apply the golden section search on the interval with tolerance equal to  $10^{-3}$  to find the accurate capacity. From Figure 6.10, we can see that the numerical results accord with the theoretical results, including various slopes and critical points.

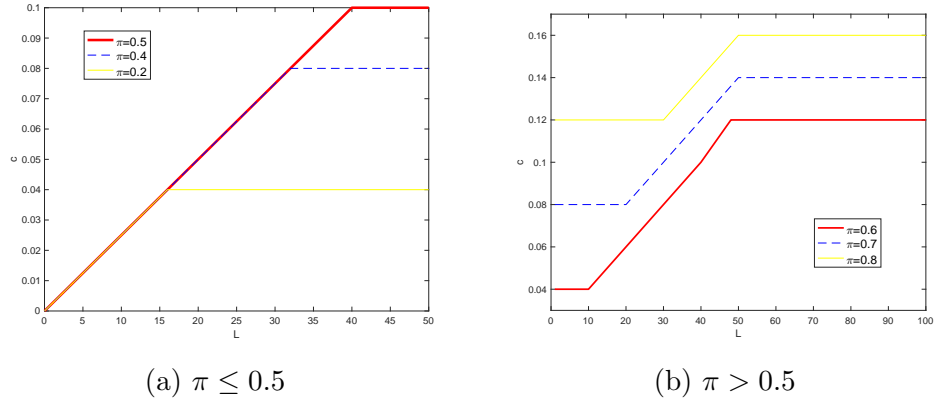


Figure 6.10: Simulated capacity of the two-signal ring road with offset

# Chapter 7

## Summary

### 7.1 Conclusion and findings

In this study, we introduce offsets to the signalized ring road to show the effects of coordinations on the performance of networks by building a rotationally symmetric N-signal ring road model with the offset  $\frac{T}{N}$  between adjacent intersections, and start with the simplest condition, the two-signal ring road model. We first derive continuous formulations for boundary flows by applying LTM and find that the two-signal ring road without offset is equivalent to the one-signal ring road both analytically and mathematically. Then we set the offset as  $\frac{T}{2}$ , and derive the approximate MFD based on two critical densities in stationery states, with the period equal to the cycle length. In addition, we also verify the capacity drop of networks due to the effect of offsets and get explicit relationships between the capacity and the ratio of the road length and the cycle length for various green ratios. Then we find the optimal cycle length for different initial conditions based on the approximate MFD by considering the effects of the lost time. To test the acquired basic theoretical results, we do various numerical simulations based on the discrete LTM. We verify the convergency



patterns for stationery states, compare the approximate MFD with simulation results, and get the system capacity under various circumstances numerically. In addition, we also find several properties of relationships between system minimum period and the cycle length.

In this study, we analyze the effects of coordinations on the signalized ring road as an supplement to the new signal design methods. We derive the new approximate MFD, analyze properties of the system capacity, and find the optical cycle length after setting offsets on the ring road. The study is a further step of the one-signal ring road model, and an important process to the N-signal ring road model.

## 7.2 Future research

### 1. Extend two-signal ring road to N-signal ring road

Now, we have a clear understanding of the two-signal ring road with a offset  $\delta = \frac{T}{2}$ , including MFD on different conditions and how the system capacity changes with the cycle length  $T$ , and find the optimal cycle length by introducing the lost time  $l$  on each phase. Since our goal is to study MFD of N-signal ring road, similarly, we can apply LTM to the N-signal ring road, get the approximate MFD and find the optimal cycle length. Then for a specific initial condition  $k_0$ , we can find the best offset  $\delta = \frac{T}{N}$  by comparing the flow-rates corresponding to the optimal cycle length of different offsets and finding the integer  $N$  that creates the maximum average flow -rate.

### 2. Set offsets to any value by changing ratio of two links' length

In the N-signal ring road, the value of offset  $\delta$  is discrete to ensure the rotational symmetry. To try different  $\delta$ , we can divide the ring road into two links with different lengths, as in Figure 7.1. The length of Link 1 and Link 2 are  $\mu L$  and  $(1 - \mu)L$ , respectively,  $\mu \in (0, 1)$ ,

then the offset  $\delta_1$  from Signal 2 to Signal 1 and the offset  $\delta_2$  from Signal 1 to Signal 2 are  $\mu T$  and  $(1 - \mu)T$ , respectively. Similarly, we can apply LTM to derive MFD, and find the relationship between  $k_0$  and  $\mu$  by comparing average flow-rates of different  $\mu$ .

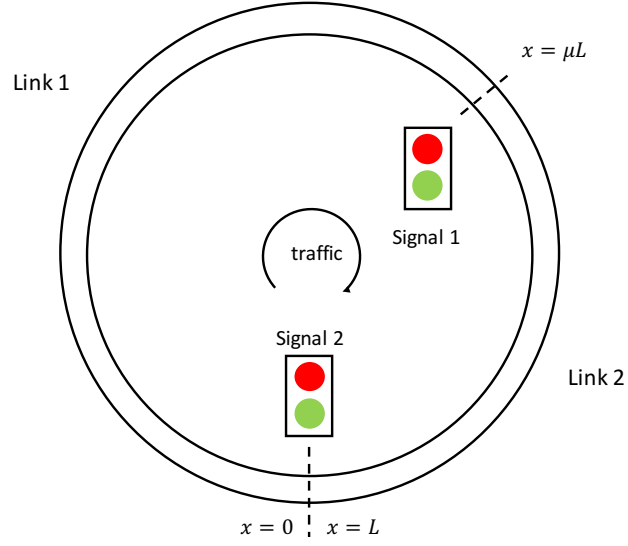


Figure 7.1: A ring road with two nonsymmetric signals

# Bibliography

- [1] C. F. Daganzo. The cell transmission model, part ii: network traffic. *Transportation Research Part B: Methodological*, 29(2):79–93, 1995.
- [2] C. F. Daganzo. A variational formulation of kinematic waves: basic theory and complex boundary conditions. *Transportation Research Part B: Methodological*, 39(2):187–196, 2005.
- [3] C. F. Daganzo. A variational formulation of kinematic waves: Solution methods. *Transportation Research Part B: Methodological*, 39(10):934–950, 2005.
- [4] C. F. Daganzo and N. Geroliminis. An analytical approximation for the macroscopic fundamental diagram of urban traffic. *Transportation Research Part B: Methodological*, 42(9):771–781, 2008.
- [5] L. Evans. Partial differential equations, grad. *Studies in Math*, 19, 1998.
- [6] N. Geroliminis and C. F. Daganzo. Existence of urban-scale macroscopic fundamental diagrams: Some experimental findings. *Transportation Research Part B: Methodological*, 42(9):759–770, 2008.
- [7] J. Godfrey. The mechanism of a road network. *Traffic Engineering and Control*, 8(8), 1969.
- [8] W.-L. Jin. Continuous formulations and analytical properties of the link transmission model. *Transportation Research Part B: Methodological*, 74:88–103, 2015.
- [9] W.-L. Jin. On the existence of stationary states in general road networks. *Transportation Research Part B: Methodological*, 81:917–929, 2015.
- [10] W.-L. Jin and Y. Yu. Asymptotic solution and effective hamiltonian of a hamilton–jacobi equation in the modeling of traffic flow on a homogeneous signalized road. *Journal de Mathématiques Pures et Appliquées*, 104(5):982–1004, 2015.
- [11] W.-L. Jin and Y. Yu. Performance analysis and signal design for a stationary signalized ring road. *arXiv preprint arXiv:1510.01216*, 2015.
- [12] M. J. Lighthill and G. B. Whitham. On kinematic waves. ii. a theory of traffic flow on long crowded roads. In *Proceedings of the Royal Society of London A: Mathematical, Physical and Engineering Sciences*, volume 229, pages 317–345. The Royal Society, 1955.

- [13] G. F. Newell. A simplified theory of kinematic waves in highway traffic, part ii: Queueing at freeway bottlenecks. *Transportation Research Part B: Methodological*, 27(4):289–303, 1993.
- [14] P. I. Richards. Shock waves on the highway. *Operations research*, 4(1):42–51, 1956.
- [15] R. P. Roess, E. S. Prassas, and W. R. McShane. *Traffic engineering*. Prentice Hall, 2004.
- [16] I. Yperman. The link transmission model for dynamic network loading. 2007.